SUPPLEMENTAL MATERIALS.

1) Supplemental Methods
2) Supplemental Tables
3) Supplemental Figures and Figure Legends
4) Supplemental References

SUPPLEMENTAL METHODS

MOUSE GENERATION

Rbm20$^{\Delta RRM}$ mice:

Targeting vector construction: Homologous recombination was used to remove exons 6 and 7 from the *Rbm20* gene resulting in an in-frame deletion of the RNA recognition motif. Homology arms were amplified from C57BL/6 genomic DNA while introducing restriction sites for use with vector Osdd (primers: short_arm_forward, CCGCTCGAGATTGAGGGCCTGCAGATATGG; short_arm_reverse, CCATCGATTTAAATGTTTGGATTCTGTGGTTGG; long_arm_forward, ACGCGTCGACCCTATCCTTGAATGCAACTTCTGG; long_arm_reverse, ATAAGAATGCGGCCGCTCTGACACAGCTGGGTTTCC). Assembly of the targeting vector replaced a 3292bp genomic DNA segment spanning exons 6-7 with a Cla I/Sal I restriction fragment containing the *loxP*-flanked *Neo* cassette.

ES cell targeting and screening: Linearized targeting vector was electroporated into white C57BL/6 ES cells. Positive selection (G418 resistance) was used to identify integration while negative selection (*TK*) was used to ensure homologous recombination. Targeted ES cells were screened by PCR (primers: RBM20.mscreenF, ATATCTGCACCCATGTTTAGTTTCC; RBM20.mscreenR, CAGAAGTTGCATTCAAGGATAGG; wild type product 3.6kb, targeted allele product 1.4kb).

Chimera generation and mouse genotyping: Targeted ES clone B6-B4 was injected into blastocysts from C57BL/6 mice. Embryos were transferred into pseudopregnant recipients and allowed to develop to term. Chimeric mice were identified by white coat color patches. Offspring from chimeras were tested for germline transmission of the targeted allele by PCR using the same primers for screening ES cells. Mice were maintained in a C57BL/6 background and periodic backcrossing was used to minimize genetic drift. Routine genotyping: PCR reactions used 1µl template {overnight tail digests: 0.1M Tris pH 8.8, 5mM EDTA, 200mM NaCl, 0.2% SDS, 0.1mg/ml Proteinase K (Worthington Biochemical Corporation) incubated overnight at 55°C} in 20µl volume using GoTaq Green Master Mix (Promega) in parallel reactions with primers P1 and P2 for wild-type or primers P1 and P3 for targeted allele {primers: P1, ATATCTGCACCCATGTTTAGTTTCC; P2, GAAGCCAGTGTGTTGGTATGG; P3 GTGGCCAGCCACGATAGC (wild-type 498bp, targeted allele 817bp)}; reactions were carried out in a C1000 Thermal Cycler (BioRad) with 39 cycles (95°C 30 sec, 60°C 30 sec, 72°C 60 sec) followed by a 10 min extension at 72°C .

Conditional *Rbm20*$^{\Delta RRM}$ mice:

Targeting vector construction: Homologous recombination was used to target the same region of *Rbm20* as the *Rbm20*$^{\Delta RRM}$ allele. The homology arms were amplified from C57BL/6 genomic DNA while introducing restriction sites for use with vector Osdd (primers: left arm forward, GGAATTCCTCGAGGGGAAGGTCTACTCTATCATTAACTCC; left arm reverse, GGCCGGCCCTACAAAGGGATTCATATTTCCAAC; middle arm forward, CCATCGATGTTGGAAATATGAATCCCTTTGTAG; middle arm reverse1, ATAACTTCGTATAATGTATGCTATACGAAGTTATACGGCTGTAAACTCCTTTCC; middle arm reverse2,

ACGCGTCGACATAACTTCGTATAATGTATGC; right arm forward, ACGCGTCGACAAGGGTGGTTTAGTTTGAAGAGG; right_arm_reverse, AAGGAAAAGCGGCCGCAGATAACCATATTTGGTGCAAACC. The targeting vector was assembled with the left arm of homology, followed by a 1589bp Fse I/Cla I restriction fragment containing *FRT*-flanked *Neo* cassette and the first *loxP* site, followed by the middle arm of homology containing the RRM-encoding exons 6 and 7 which was sequentially amplified to incorporate the second *loxP* site and a Sal I restriction site which was used to ligate the right arm of homology.

ES cell targeting and screening: Linearized targeting vector was electroporated into two ES cell lines (129P2 and 129S6). Positive selection (G418 resistance) was used to identify integration and screened by PCR reactions for recombination at each end. Multiple positive clones were identified from each cell line.

Chimera generation and mouse genotyping: Targeted ES clones from each cell line were injected into blastocysts from C57BL/6 mice. Embryos were transferred to pseudopregnant recipients and allowed to develop to term. Chimeric mice were identified by coat color. Offspring from chimeras were tested for germline transmission of the targeted allele by PCR using primers (cRBM20_F, ACAACTCCCACTAGCTGTGTATGG; cRBM20_KO_R, GAAACACGGAAGGAGACAATACC; cRBM20_WT_R, CAAACTGATGGGACAAAGAGC; WT product 280bp, targeted allele 460bp).

Confirmed *Rbm20*$^{\Delta RRM\ flox}$*/+* mice were crossed to *FLPe* mice (B6;SJL-Tg(ACTFLPe)9205Dym/J strain from Jackson Laboratory) to remove the *Neo* cassette. Offspring were screened for removal of *Neo* by PCR (primers cRBM20_F and cRBM20_WT_R, WT product 280bp, targeted allele without neo 410bp). Mice were then backcrossed to C57BL/6J multiple generations. To produce the cardiac-specific conditional allele *α-MHC Cre mice* {*B6.FVB-Tg(Myh6-cre)2182Mds/J* strain (Jackson Laboratory)} were crossed to *Rbm20*$^{\Delta RRM\ flox}$*/+* mice. Mice were housed in a pathogen-free vivarium with 12hr light:12hr dark cycle.

ECHOCARDIOGRAPHY

Anesthesia was induced by intraperitoneal (i.p.) injection of ketamine hydrochloride (K2753, Sigma-Aldrich) 100 mg/kg plus atropine sulfate (A0257, Sigma-Aldrich) 1.2 mg/kg. Following anesthetic induction, the mouse was placed in dorsal recumbence on a heated platform for echocardiography. Body temperature was maintained at 37°C and anesthesia was maintained with 0.5-1.0% isoflurane (USP, Phoenix) in 100% oxygen. Transthoracic echo images was obtained with a Vevo 700 High Resolution Imaging System (Visual-Sonics, Toronto, Canada) using the model 707B scan head designed for murine cardiac imaging. Care was taken to avoid animal contact and excessive pressure which could induce bradycardia. Imaging was performed at a depth setting of 1 cm. Images were collected and stored as a digital cine loop for off-line calculations. Standard imaging planes, M-mode, Doppler, and functional calculations were obtained according to American Society of Echocardiography guidelines. The parasternal long axis view and mid wall cross sectional view of the left ventricle (LV) were used to guide calculations of percentage fractional shortening, percentage ejection fraction, and ventricular dimensions and volumes. In addition, the left atrial dimension was measured in the long-axis view

directly below the aortic valve leaflets. Passive LV filling peak velocity, E (cm/sec), and atrial contraction flow peak velocity, A (cm/sec), were acquired from the images of mitral valve Doppler flow from tilted parasternal long axis views. A sweep speed of 100 mm/sec was used for M-mode and Doppler studies. Considering that heart rate positively correlates with systolic performance, the heart rate of animals during echocardiographic study were maintained in the range of 500 -550 beats/min for M-mode, 450-500 beats/min for B-mode and 350 to 450 beats/min for Doppler studies.

Conscious echo and Stress testing. A separate group of mice were consciously echoed while scruffing the skin at the nape of the neck and a standard short axis (M-mode) cine loop was recorded at the level of the papillary muscles to asses chamber dimensions (LV systolic and diastolic dimensions (LVDs, LVDd)) posterior wall thickness (PWT), and cardiac function via fractional shortening (%FS). Data was analyzed in Vevo770 3.0 software suite (VisualSonics). After recording baseline measurements, mice were given an i.p. injection of phenylephrine (P6126, Sigma-Aldrich) 1.0 mg/kg diluted in 0.9% saline[1] and 4 min after injection a cine loop was recorded.

TISSUES COLLECTION

Mice were weighed, anesthetized with isoflurane and sacrificed by cervical dislocation. The hearts were rapidly excised and placed into a dish containing HEPES buffer ([in mmol/L] 133.5 NaCl, 5 KCl, 1.2 NaH_2PO_4, 1.2 $MgSO_4$, 30 BDM, 10 HEPES). All four chambers were removed, blotted and weighed separately. The left ventricle (LV) was further separated into 2 sections, one of which was snap frozen in liquid nitrogen and the other placed into RNALater for subsequent analysis. Tibias were removed and tibia length was measured using a caliper.

QUANTIFICATION OF PROTEIN EXPRESSION

Flash-frozen LV tissues were prepared as previously described[2-4]. Briefly, the LV tissues were flash frozen in liquid nitrogen and solubilized between glass pestles cooled in liquid nitrogen. Tissues were primed at -20^{o}C for a minimum of 20 min, then suspended in 50% urea buffer ([in mol/L] 8 Urea, 2 Thiourea, 0.05 Tris-HCl, 0.075 Dithiothreitol with 3% SDS and 0.03% Bromophenol blue pH 6.8) and 50% glycerol with protease inhibitors ([in mmol/L] 0.04 E64, 0.16 Leupeptin and 0.2 PMSF) at 60^{o}C for 10 min. Then the samples were centrifuged at 13000 rpm for 5 min, aliquoted and flash frozen in liquid nitrogen and stored at -80^{o}C.

Titin isoform analysis was performed as previously described [4]. Briefly, the solubilized samples from each genotype (LV of *Rbm20*$^{\Delta RRM}$ +/+ (WT), +/- (Het), and -/- (Hom)) were electrophoresed on 1% agarose gels using a vertical SDS-agarose gel system (Hoefer). Gels were run at 15 mA per gel for 3 h and 20 min, then stained using Coomassie brilliant blue (Acros organics), scanned using a commercial scanner (Epson 800, Epson Corporation, Long Beach CA) and analyzed using One-D scan (Scanalytics Inc, Rockville MD). Each sample was loaded in a range of five volumes and the integrated optical density (IOD) of titin and MHC were determined as a function of loading volume. The slope of the linear relationship between IOD and loading was obtained for each protein to quantify expression ratios. Expression levels were also quantified from LV of +/+, +/-, and -/- with western blotting as previously described [5]. Solubilized samples were run on a 0.8% agarose gel in a vertical gel electrophoresis chamber. Gels run at 15 mA per gel for 3 h and 20 min were then transferred onto PVDF membranes

(Immobilon-FL, Millipore) using a semi-dry transfer unit (Trans-Blot Cell, Bio-Rad, Hercules CA). Blots were stained with Ponceau S (Sigma) to visualize the total protein transferred. Blots were then probed with primary antibodies (see Table 1) followed with secondary antibodies conjugated with fluorescent dyes with infrared excitation spectra (Biotium Company, Hayward CA). Blots were scanned using an Odyssey Infrared Imaging System (Li-COR Biosciences, Lincoln NE) and the images were analyzed using Li-COR software. Ponceau S scans were analyzed in One-D scan to normalize WB signal to protein loading. A list of primary antibodies used in western blot studies is provided is shown below.

Antibody	Source	Host	Dilution
αRBM20	Gift from Dr.Gotthardt, MDC Berlin (Details in [6]).	Rabbit	1:500
αN2B	Anti I24-I25 N2B N-term x214-x215 (Details in [7]). Gift from Dr.Labeit Mannheim University (available from www.myomedix.com)	Rabbit	1:500
αTMOD	EMOD, Gift from Dr.Gregorio, University of Arizona.	Rabbit	1:600
α9D10	Developmental Studies Hybridoma Bank (DSHB), University of Iowa(details in [8]).	Mouse	1:1500
αN2A	Anti x105-x106 (details in [7]). Gift from Dr.Labeit, (available from www.myomedix.com)	Rabbit	1:500
αNovex III	Gift from Dr.Labeit (details in [9]). (available from www.myomedix.com)	Rabbit	1:500
αLDB3	Novus Biologicals	Rabbit	1:800
αNCX-1	Santa Cruz Biotechnology	Rabbit	1:200
αSERCA2a	Badrilla	Rabbit	1:2500
αPLBT17	Badrilla	Rabbit	1:1500
αPLB	Badrilla	Mouse	1:1500
αpS282 cMyBP-C	Enzo Life Sciences	Rabbit	1:2500
αMyBP-C	Santa Cruz Biotechnology	Mouse	1:500
αcTnT	Santa Cruz Biotechnology	Mouse	1:200
αcTm	Santa Cruz Biotechnology	Mouse	1:200
αpS23/24 TnI	Cell Signaling	Rabbit	1:500
αcTnI	Santa Cruz Biotechnology	Mouse	1:200
αcMLC2v	Santa Cruz Biotechnology	Goat	1:3000
αGAPDH	Thermo Pierce	Mouse	1:2500
p53	Millipore	Mouse	1:1000
αCaMKIIδ	ABCAM	Rabbit	1:250

Myosin isoform analysis was performed using 7% acrylamide gels as previously described[10]. Briefly, solubilized LV samples of +/+, +/-, and -/- were loaded onto vertical gel electrophoresis chambers with a 4% acrylamide stacking layer and 7% acrylamide resolving layer. Gels were run at 275 V for 24 h at 12°C. Gels were stained with Coomassie brilliant blue because it binds stoichiometrically to proteins, has a wider dynamic range and a wider linear relationship between quantity of protein and staining intensity vs. silver stain. Gels were then scanned and analyzed using One-D scan software. Each sample was loaded one time in sets of 3 in a row (+/+, +/- and -/-).

Thin and thick filament regulatory proteins expression and phosphorylation were analyzed as previously described [3, 11-13]. Briefly, LV samples from all three genotypes were loaded onto a 12% SDS-

PAGE gel and run for 2 h at 100 V. Gels were fixed in 50% methanol, 10% acetic acid overnight then stained with Pro-Q Diamond Phosphoprotein Gel stain (Invitrogen), destained with 20% acetonitrile, 50 mM sodium acetate pH 4, and scanned with a 302 nm UV transilluminator (G: BOX Syngene, USA). Gels were then stained with Coomassie brilliant blue, scanned, and analyzed using One-D scan for protein content. Each sample was loaded one time in sets of three in a row.

RNA ANALYSIS

Custom *Titin* Exon Microarray. *Ttn* mRNA expression was analyzed using our custom exon microarray as previously described [2, 12, 14, 15, 16]. Left ventricular tissues were dissected from male mice (4 month-old) and stored in Ambion RNAlater (Invitrogen). Total RNA was isolated using the Qiagen RNeasy Fibrous Tissue Mini Kit (Qiagen). The SenseAmp Kit (Genisphere) and Superscript III reverse transcriptase enzyme (Invitrogen) were used for sense amplification of each sample. Samples of the same genotype were pooled for reverse transcription and dye-coupled with Alexa Fluor 555 and Alexa Fluor 647 using the SuperScript Plus Indirect cDNA Labeling System (Invitrogen). A 3-point hybridization loop design with technical replicate dye-flip was used; 750 ng of labeled cDNA with each fluorophore were co-hybridized on individual slides (platform: 50-mer oligonucleotides specific for each *Ttn* exon robotically spotted in triplicate on Corning Ultra GAPS slides) using SlideHyb Buffer #1 (Ambion) in a GeneTAC Hybridization Station (Genomic Solutions) for 16 h at 42°C. Slides were scanned at 595 nm and 685 nm with an ArrayWoRx scanner (Applied Precision). Spot-finding was performed with SoftWoRx Tracker (Applied Precision) and analyzed with the CARMA package [17].

GeneChip. Left ventricular tissue was dissected from four 6.5 week-old male mice for each *Rbm20*$^{\Delta RRM}$ genotype (+/+, +/- , -/-) and stored in Ambion RNAlater (Invitrogen). Total RNA was isolated using the Qiagen RNeasy Fibrous Tissue Mini Kit (Qiagen). RNA quality was assessed by NanoDrop 1000 Spectrophotometer and 2100 Bioanalyzer (Agilent); all samples had RIN≥9.2. Samples were hybridized with the Mouse Exon 1.0ST Array (Affymetrix); processing (labeling through scanning) was performed by the Genomics Core, The University of Arizona, following Affymetrix protocols and using Affymetrix supplies and equipment. Data analysis was conducted using the Exon Array Analyzer server (http://eaa.mpi-bn.mpg.de/) [18]. PLIER was used with the full gene set since neither TTN nor RBM20 probesets are present in the core or extended gene sets. The EAA implementation of DABG with recommended filter settings (including Benjamini-Hochberg correction for multiple testing) was used; Limma was used for analysis at both the exon level and gene level. Changes in splicing were identified by Splicing Index absolute value ≥2[19], and an adjusted *p*-value of ≤0.05 (probesets with an average intensity less than twice background were removed); changes in gene expression level were identified by an adjusted *p*-value of ≤0.05. WebGestalt (http://bioinfo.vanderbilt.edu/webgestalt/) was used to identify over-representation among spliced gene targets by GO analysis, KEGG analysis, WikiPathway analysis; however none was identified[20, 21].

RT-PCR.

Total RNA was extracted using the RNeasy Fibrous Tissue Mini Kit with DNase treatment (Qiagen) from left ventricle tissue which upon dissection had been immediately immersed into RNAlater

(Ambion) and stored at -20°C. Samples were from four 6.5-week-old male mice of each genotype (+/+, +/-, -/-) or three 6.5-month-old male rats of each genotype (+/+, -/-). SuperScript III (Invitrogen) was used to reverse transcribe total RNA; cDNA equivalent to 25ng total RNA were used for each reaction.

Quantitative RT-PCR used Maxima SYBR Green qPCR Master Mix (Fermentas) in a Rotor-gene 6000 (Corbett Life Science), Endpoint RT-PCR analysis used GoTaq Green Mastermix (Promega) in C1000 Thermocycler (Bio-Rad) and analyzed in agarose gel visualized with ethidium bromide. Primer sequences are found in table 2; rat primer sequences for RBM20 splicing targets are from Guo et al. (2012) and corresponding mouse primer sequences were selected based upon corresponding exon locations of the rat primers.

Quantification of *Cypher/Ldb3* was performed with *Polr2a* as the reference gene using the $\Delta\Delta C_T$ method (primers: mLdb3.F, CAACCCCATTGGCCTGTACT; mLdb3.R, CACAGGGAGGCTCCCTCCT; mPolr2a.R, GGATCCATTAGTCCCCCAAG; mPolr2a.L, TCAAGAGAGTGCAGTTCGGA); specificity of qPCR products was confirmed by melting point analysis. A list of primer sequences is given below.

Target	Rat		Mouse	
	Primers	Products	Primers	Products
Rbm20 exon2	For: 5'-CAGCCTGCCCCAGATCAT-3' (ex1) Rev: 5'-CCATCTTCAGCCGATGGA-3' (ex2)	149bp	For: 5'-CAGCCTGCCCCAGATCAT-3' (ex1) Rev: 5'-CTGGCGACGTGAGCAGAG-3' (ex2)	92bp
Rbm20 exon6	For: 5'-ATATGCAGCCATTCCAACAAG-3' (ex5) Rev: 5'-GCAGATGTGCACAACTCGTC-3' (ex6)	118bp	For: 5'-ATATGCAGCCATTCCAACGA-3' (ex5) Rev: 5'-GATGTGCACTACCCGTCCAG-3' (ex6)	115bp
Cypher/Ldb3	For: 5'-TCCAAGCGTCCTATCCCCATC-3' * Rev: 5'-TGTATTCTGTCCCGGTCATCTG-3' *	614bp ~510bp 488bp ~425bp ~295bp	For: 5'-TCCAAGCGGCCTATTCCCATC-3' Rev: 5'-TGTATTCTGTCCCGGTCATCTG-3'	604bp 472bp
Camk2delta	For: 5'-AAGGGTGCCATCTTGACAAC-3' * Rev: 5'-TCGAAGTCCCCATTGTTGAT-3' *	311bp 260bp 233bp 200bp	For: 5'-AAACTGAAGGGCGCCATCTT-3' Rev: 5'-GCCTCAAAGTCCCCATTGTTGAT-3'	311bp 269bp 242bp 209bp
Camk2gamma	For: 5'-CAACGGTCAACAGTGGCATCC-3' * Rev: 5'-GTGTAGGCCTCAAAGTCCCCA-3' *	~450bp 410bp 341bp	For: 5'-AAGGGTGCCATCCTCACAAC-3' Rev: 5'-GTGTAGGCCTCAAAGTCCCCA-3'	~430bp 362bp 329bp 293bp 260bp
Sh3kbp1	For: 5'-GTGGAGGAAGGATGGTGGGAA-3' * Rev: 5'-CCACTTCAATCGACCTTGGTC-3' *	442bp 367bp 310bp	For: 5'-ACGATGAGCTGGAGCTGAAA-3' Rev: 5'-TCCACTTCAATCGACCTTGG-3'	361bp ~280bp
Sorbs1	For: 5'-CTTTCAGAATGTGATGTTGGAAG-3' * Rev: 5'-CTGACTTGTTTTCATGCTTCG-3' *	~510bp 295bp 205bp	For: 5'-AAGCTGTGGTGAATGGCTTG-3' Rev: 5'-TGACTTGCTTTCATGCTTCG-3'	266bp 176bp
Trdn	For: 5'-CAGAGACAAAGATGGCAGCAA-3' * Rev: 5'-CTTCCAGTGATGGTGTTGACA-3' *	339bp 279bp	For: 5'-GAGACGAAGATGATGGCAAAA-3' Rev: 5'-TGGCATAACTGGGCTTTGTC-3'	279bp

*primers from Guo *et al.* (2012)

CARDIOMYOCYTE STUDIES

Cell isolation. Cells were isolated as described previously[22]. Briefly, mice were heparinized (1,000 U/kg, i.p.) and euthanized by cervical dislocation under isoflurane. The heart was removed and cannulated via the aorta with a blunted 21-gauge needle for retrograde coronary perfusion. The heart was perfused for 4 min with perfusion buffer ([in mmol/L] 113 NaCl, 4.7 KCl, 0.6 KH_2PO_4, 0.6 Na_2HPO_4, 1.2 $MgSO_4$, 12 $NaHCO_3$, 10 $KHCO_3$, 10 HEPES, 10 taurine, 5.5 glucose, 5 BDM, 20 Creatine, 5 Adenosine and 5 Inosin, pH 7.4), followed by digestion buffer (perfusion buffer plus 0.05 mg/ml Liberase TM research grade; Roche Applied Science, and 13 µM $CaCl_2$) for 20 min. When the heart was flaccid, digestion was halted and the heart was placed in myocyte stopping buffer (perfusion buffer plus bovine calf serum 0.08 [BCS]/ml and 8 µM $CaCl_2$) with protease inhibitors ([in mmol/L] 0.4 Leupeptin, 0.1 E64, and 0.5 PMSF (Peptides International,Sigma-Aldrich)). The left ventricle was cut into small pieces, and

the rest of the heart was discarded. The small pieces of left ventricle were triturated several times with a transfer pipette and then filtered through a 300μm nylon mesh filter.

Skinned cells-general. Mouse cells, isolated as explained above, were skinned for 7 min in relaxing solution ([in mmol/L] 40 BES, 10 EGTA, 6.56 $MgCl_2$, 5.88 Na-ATP, 1.0 DTT, 46.35 K-propionate, 15 creatine phosphate, pH 7.0) with protease inhibitors ([in mmol/L] 0.4 leupeptin, 0.1 E64 , and 0.5 PMSF) and 0.3% Triton X-100 (Ultrapure; Thermo Fisher Scientific). Cells were washed extensively with relaxing solution pCa 9 and stored on ice. Skinned myocytes were used for mechanic studies within 48 h after time of cell isolation. Myocyte suspension was added to a room temperature flow-through chamber mounted on the stage of an inverted microscope (Diaphot 200; Nikon). Skinned myocyte was glued at one end to a force transducer (Model 406A or 403A, Aurora Scientific). The other end was bent with a pulled glass pipette attached to micromanipulator so that the myocyte axis aligned with the microscope optical axis and cross sectional area (CSA) was measured directly. The cross sectional images of skinned cells were analyzed by ImageJ 1.41 software (National Institutes of Health) and were used to convert measured force to stress and for cell dimension study (Fig S4d). Then, the free end of the cell was glued to a servomotor (Model 308B, Aurora Scientific) that imposes controlled stretches. Sarcomere length (SL) was measured with a MyocamS and SarcLen acquisition module (IonWizard 6.2, IonOptix Co, MA) attached to a computer. To correct for ~20% lattice expansion during skinning process[23], CSA of skinned cells were divided by a correction factor of 1.44.

Passive stress in skinned myocytes. Passive stress was measured in relaxing solution pCa 9 with protease inhibitors at room temperature. Cells were stretched from slack length at a speed of 1 base length/sec to a SL of 2.3 μm for +/+, 2.7 μm for +/- and 3.0 μm for -/-, followed by a 20 sec hold and then a release back to the original length. Recovery time of at least 7 min in between stretches was utilized to prevent memory-effects in subsequent measurements. Data were collected using a custom LabVIEW VI (National Instruments, Austin TX) at a sample rate of 1 kHz. Measured forces were converted to stress (force/unit undeformed CSA). The stress during the 1 base length/sec stretch was plotted against the SL and fitted with a monoexponential curve to derive stress-SL relationships.

Maximal activated stress in skinned myocytes. Cell in relaxing solution pCa 9 was glued to force transducer and servomotor as described. Activation was carried out at temperature 20°C by perfusion activating solution pCa 4.5 ([in mmol/L] 40 BES, 10 Ca-EGTA, 6.29 $MgCl_2$, 6.12 Na-ATP, 1 DTT, 45.3 potassium-proprionate, 15 creatine phosphate) plus protease inhibitors in to the temperature controlled chamber. Cells with slack SL shorter than 2.0 μm were stretched to SL 2.0 μm, whereas cells with slack SL longer than 2.0 μm were buckled to SL 2.0 μm, therefore cells of all genotypes were activated at SL 2.0 μm. After the activated stress reached a plateau, the solution was switched back to relaxing solution pCa 9.

Intact cells-general. Intact cardiomyocytes were isolated as described above, then Ca^{2+} was reintroduced to cardiomyocyte suspension to a final concentration of 1 mM. An inverted microscope (IX-70; Olympus) was used with a chamber that had platinum electrodes to electrically stimulate cells and a perfusion line with heater control and suction out to maintain a flow rate of ∼2 ml/min. All intact cell experiments were performed at temperature 37°C in MEM Alpha (12000, Gibco, Life Technologies) plus 10 μg/mL insulin (I9278,Sigma-Aldrich). Cells were field-stimulated at 2 Hz frequency by MyoPacer

stimulator (IonOptix Co, MA). All images were recorded with X40 objective lens. Data were collected using an IonOptix FSI A/D board and IonWizard 6.2.2.61 software (IonOptix Co, MA) with SarcLen and SoftEdge modules to determine SL and carbon fiber displacement. The sampling frequency of the system was sufficient to measure force (1,000 Hz) and SL (250 Hz) simultaneously.

Intact cells--unloaded. Shortening and relengthening of sarcomere length were recorded. Steady state twitches (10-20) of isolated cardiomyocyte were averaged and the transient parameters were obtained from monotonic transient analysis. The baseline, transient amplitude, maximal departure velocity and maximal return velocity of SL were defined.

Intact cells--loaded. Carbon fibers (10 µm cfs; b-1; TMIL Ltd.) were used to attach to cells, stretch the cells, and measure force[24]. Carbon fibers were mounted in custom-pulled and angled glass pipettes (0.7–1.2 mm of carbon fibers protruding from pipette tip), and their stiffness was determined by cross-calibrating with a force transducer (model 406A; Aurora Scientific). The carbon fiber was displaced by the force transducer to ∼10 different lengths, and then force versus displacement was plotted to determine the slope (stiffness) of each carbon fiber previous to use. Stiffness ranged from 0.05-0.15 µN/µm, giving rise to a force resolution of 0.005-0.015 µN. Cells were attached to carbon fibers as described previously [25]. Briefly, a strongly contracting rod-shaped cell was selected, and the carbon fibers coated with MyoTak (IonOptix Co, MA) were carefully lowered onto opposite ends of the cell. The cell was slightly pressed between the coverslip and the carbon fibers, and once attached, the cells were lifted off the coverslip. These manipulations resulted in small changes in cell length and the baseline SL of cells attached to carbon fibers deviated slightly from the baseline SL of unloaded cells (Fig 1 and Table S4). The carbon fiber movement was controlled via custom LabVIEW software through piezo motion controller (E-503; Physik Instrumente). All forces were normalized to stress. Cross sectional area of intact cell was obtained from the measured cell width assuming that the cross section of the cell was an ellipse [26]. The experimentally determined cellular thickness/width ratios of +/+ and +/- were both 0.34±0.02 while this ratio of -/- was 0.41±0.03. In addition we also studied intact cells and found a width:thickness ratio of 0.34 ±0.01 in +/+, 0.35 ±0.01 in +/- while in -/- the ratio was 0.41±0.01. ANOVA with a post-hoc Bonferoni test corrected for multiple comparisons showed that there were no significant differences in the width:thickness ratio between intact and skinned cells and that the ratio between -/- and +/- and between -/- and +/+ cells was significantly different (p<0.001) in both skinned and intact cells. The CSA of +/+ and +/- cells were calculated as $\pi \times (Width/2) \times (width/(2 \times 0.34))$, and for -/- cells as $\pi \times (Width/2) \times (width/(2 \times 0.41))$.

Stretch-release protocol for loaded intact cells. To determine diastolic stress, stretch-release protocol was applied during a prolonged diastolic interval. Cell attached to carbon fibers was activated at 2 Hz, then the pacing was paused for 1 sec and the stretch was imposed at 1 base length/sec to SL(s) 2.15 µm for +/+, 2.35 µm for +/- and 2.55 µm for -/-, then cell was released back to baseline and twitch activation was resumed. To inhibit diastolic crossbridges, cells were perfused with 20 µM blebbistatin (B0560, Sigma-Aldrich)[27]. Cells perfused with blebbistatin had a red filter over the light source to prevent breakdown of blebbistatin. After the cell was exposed to inhibitor, a reduction in twitch force and SL shortening occurred within seconds. A complete cessation of contractility occurred within ~100 sec and a new baseline was established. Stretch was imposed again at approximately 420 sec after initiation of

blebbistatin infusion. Differences of diastolic stress before and after crossbridge inhibition were used as a measurement of diastolic crossbridges.

Stretch-hold-release protocol for loaded intact cells. To determine the Frank-Starling mechanism (FSM), a stretch-hold-release protocol was used. The cell was rapidly stretched during diastole with ramp time 300 msec, then held at constant length until a twitch was completed. During the stretch and subsequent hold the cell developed diastolic stress in addition to active stress during the twitch. The cell was then released back to the base length and after 100 contractions (to establish a steady-state) the stretch was repeated but to a different length. The stretch length was gradually increased by approximately 10 μm at a time, from 10 μm up to 50 μm or until cell was detached from the carbon fibers. The peak force of the immediate post-stretch twitch was measured. The carbon fibers measure the total force and during systole this total force consists of titin-based force and actomyosin-based force (or active force). Because titin functions as a bi-directional spring[28], above the slack sarcomere length titin develops passive force that pulls on the Z-disks (as does active force), but below the slack sarcomere length titin pushes out on the Z-disks (opposing active force) and develops the so-called restoring force. Hence to determine the active force level at sarcomere lengths above the slack length, the passive force was *subtracted* from the total force, but below the slack sarcomere length the restoring force was *added* to the total force. Systolic stresses were plotted against systolic SLs. Slopes of the systolic stress-systolic SL and systolic stress-diastolic SL relation were calculated from linear fits and used as measurements of FSM of individual cell. Slope value of -/- was normalized by percent difference between maximal activated stress of +/+ versus -/- (see text). The maximal active stress and FSM measurements were performed in different batches of cells. Propranolol administration: A separate group of mice were injected with propranolol hydrochloride (P0884, Sigma-Aldrich) 20 μg/gm bodyweight i.p. at 14 h and 2 h before euthanasia and 2 μM propranolol was added into all cell solutions.

MEASUREMENT OF CA^{2+} TRANSIENT IN INTACT CARDIOMYOCYTES

Measurement of Ca^{2+} in unloaded intact cardiomyoctyes. Isolated LV cardiac myocytes were incubated with Fura-2 AM 1 μm (F-1225, Life Technologies) in stopping buffer(perfusion buffer plus bovine calf serum 0.08 mg/ml buffer and 1 mM $CaCl_2$) for 10 min at room temperature and resuspended in 1.8 mM Ca^{2+} MEM alpha (12000, Gibco, Life Technologies). Fluorescence was measured ratiometrically with the Ion Optix photometry system (IonOptix Co, MA). Fura-2 was excited alternately at 340 and 380 nm, and emission was recorded at 510 nm. Background fluorescence was subtracted for each excitation wavelength. Ratio of fluorescence intensities excited at 340 nm and 380 nm was used as a relative measurement of cytoplasmic Ca^{2+}, the ratio transient was fitted by monotonic transient analysis software (IonWizard 6.2.2.61). All measurements were carried out at 37°C.

Measurement of Ca^{2+} transients in response to stretch. Cell was attached to carbon fibers and was stretched by 10% of the baseline length. Sarcomere length, force and fluorescence transient were recorded simultaneously. Fura-2 ratio transients (340/380 nm) of pre-stretch twitch and immediate post-stretch twitch were used for a comparison.

IN VIVO PRESSURE-VOLUME RELATIONSHIPS

In vivo pressure volume analysis was performed in mice using a SciSense Advantage Admittance Derived Volume Measurement System and 1.2F catheters with 4.5 mm electrode spacing (SciSense, London, Ontario, Canada). Mice were anesthetized and ventilated with 1% isoflurane using an SAR-1000 Ventilator (CWE Inc) and body temperature maintained at 37°C using a TC-1000 Temperature Controller (CWE Inc). Four month old anesthetized mice were secured and a midline incision was made down the neck. The muscles in the neck were separated and the right carotid artery was isolated from the vagus nerve. The right carotid artery was cannulated and the catheter guided past the aortic valve. The abdomen was opened below the sternum; the IVC was located and occluded during a sigh (pause) in ventilation to acquire load-independent indexes. Data acquisition and analysis was performed in LabScribe2 (iWorx, Dover NH). PV data was analyzed using a monoexponential fit ($P = Ae^{\beta V}$)[29] with the exponent (β) reported as the stiffness.

TAIL CUFF BLOOD PRESSURE MEASUREMENT

Mice underwent blood pressure analysis utilizing Hatteras Instruments Blood Pressure Analysis Systems (Model MC4000) placing individual tails in small cuffs, gently taping the tail and placing a magnetic cover over each mouse allowing for proper measurements to be taken. Selected mice were conditioned two consecutive days prior to final analysis by taking the measurements at the same time of the day in order to allow for mice to become accustomed to the test. Analysis included five preliminary and ten measurement cycles holding a constant temperature of 90°F with a maximum cuff pressure of 200 mmHg. Conditioning the mice allowed for stable blood pressure measurements to be taken with low errors (at least 7/10 measurement cycles completed successfully

HISTOLOGY

Hearts were obtained from anesthetized mice and were quickly cannulated. Hearts were perfused with a Ca^{2+} free Tyrode solution with 2,3-Butanedione monoxide (BDM) and KCl to maximize relaxation ([in mmol/L]25 $NaHCO_3$, 30 KCl, 118 NaCl, 1.2 $MgCl_2$, 1.2 NaH_2PO_4, 5 Glucose, 5 Na-Pyruvate, with 5 U/L Insulin and 80 mg/L Bovine Serum Albumin [BSA], 30 BDM). A 4-0 silk suture was advanced through the mitral valve and apex and left in place to eliminate fluid buildup in the ventricle. After 5 min perfusion was rapidly exchanged with a 10% formalin solution (HT5014, Sigma-Aldrich) and allowed to perfuse for 10 min. These partially fixed hearts were then removed, sliced radially in 4 sections and post-fixed in 10% formalin for 24 h. Short-axis cross sections were embedded, sectioned and stained using Picrosirius Red to quantify collagen content[30]. Stained sections were then imaged on a Zeiss microscope (Imager.M1), and analyzed for collagen volume fraction (CVF) using custom Axiovision scripts.

MEASUREMENT OF COLLAGEN STIFFNESS of LEFT VENTRICULAR FREE WALL

Mice were placed under isoflurane anesthesia, cervically dislocated, and the ribcage was rapidly removed to access the heart. One ml of HEPES pH 7.4(in mM: NaCL, 133.5; KCl, 5; NaH_2PO_4, 1.2; $MgSO_4$, 1.2; HEPES, 10) solution containing 30μM KCl and 30 mM BDM was injected into the LV through the apex, after which time the heart noticeably relaxed and ceased pumping. The heart was removed and the LV was isolated from the other chambers. The apex and base were removed from the LV leaving a cross sectional slice approximately 2mm thick. The septum and RV attachment regions were discarded

and the LV free wall tissue was placed in relaxing solution. Endocardial fibers (apical to base orientation) were dissected and discarded. Once visualized, 400μM mid-myocardial fibers (circumferential orientation) were carefully removed and skinned in fresh relaxing solution pH 7.0 with 1% Triton-X-100 (Pierce, IL, USA) overnight at ~3°C and protease inhibitors (phenylmethylsulfonyl fluoride (PMSF), 0.5 mM; leupeptin, 0.04mM; E64, 0.01mM), then washed for one hour with relaxing solution. Immediately following the wash with relaxing solution, 150-250 μm strips were dissected and aluminum clips were placed on both ends of the preparation. The aluminum clips were attached to a strain gauge force transducer and high-speed length motor and the preparation was submersed in relaxing solution. The width and the height of the fiber were determined as described as for the LDA experiment in order to determine CSA. Sarcomere length (SL) was measured on line by laser diffraction. Relaxed fibers were stretched (100%/sec) from their slack length to sarcomere lengths of 2.0, 2.1, 2.2, and 2.3 μm with a 12 minute rest between stretches. To determine the collagen contribution to passive force, thick and thin filaments were extracted from the sarcomere, removing titin's anchors in the sarcomere. Collagen based stress-strain relation was fit with equation $\sigma = E_o/\alpha[e^{(\epsilon\alpha)}-1]$, where σ=passive stress, E_o= the initial elastic modulus, α= empirical constant, and ϵ=strain $(SL / SL_0 - 1.0)$[31].

LENGTH DEPENDENCE OF ACTIVATION OF FORCE DEVELOPMENT

Mice were anesthetized with isoflurane and sacrificed by cervical dislocation. The hearts were rapidly removed; papillary muscles from the LV were dissected in oxygenated HEPES ([in mmol/L] 133.5 NaCl, 5 KCl, 1.2 NaH_2PO_4, 1.2 $MgSO_4$, 30 BDM, 10 HEPES) solution and then skinned in relaxing solution with 1% Triton X-100 for overnight at ∼3 °C. Muscles were then washed thoroughly with relaxing solution and stored at −20 °C in relaxing solution containing 50% (v/v) glycerol. To prevent protein degradation, all solutions contained protease inhibitors ([in mmol/L] 0.01 leupeptin, 0.04 E64, and 0.5 PMSF). Skinned papillary muscles were dissected into small strips (CSA ∼0.02 mm^2; length∼1.2 mm) and small aluminum clips were glued to the ends of the muscle[32] in order to attach the muscle at one end to a force transducer (model 406, Aurora Scientific) and at the other end to a length controller (model 322C, Aurora Scientific),which were mounted on top of an inverted microscope stage. The stage contained 6 wells with different solutions in which the muscles could be placed (model 600A, Aurora Scientific). The muscles were imaged with a CCD camera, and sarcomere length was measured online from the striation image using a spatial autocorrelation function (model 901, Aurora Scientific). The wells were temperature controlled at 15°C. Thickness and width of the preparation were measured and CSA was calculated assuming an elliptical cross-section. The CSA was used to convert measured force into stress.

LDA study . Relaxing solution (RS), pre-activating solution (Pre-A), and maximal activating solution (AS) were utilized. All solutions contained: [in mmol/L] 40 BES, 1 DTT, 33 creatine phosphate, creatine phosphokinase (CPK) 240 U/ml; the ionic strength was adjusted to 180 mM with K-proprionate; pH 7.0 at 15 °C. In addition we used $MgCl_2$ 6.86, 6.66 and 6.64; Na-ATP 5.96, 5.98, and 6.23; EGTA, 10, 1 and 0.0; Ca-EGTA 0.0, 0.0, and 10.0; k-proprionate 3.28, 30.44, and 2.09 in Relaxing, Pre-activating and

Activating solutions, respectively. Submaximal activating solutions were obtained by mixing RS and AS with the free [Ca^{2+}] calculated according to Fabiato and Fabiato[33].

Fibers were set at a SL of 1.91, 2.05 and 2.15 µm for +/+, +/- and -/-. The fibers were activated in the following sequence: pre-activating solution, pCa 4.5, relaxing solution, pre-activating solution, pCa 6.05, 5.85, 5.75, 5.6, and 4.5, relaxing solution. The pCa 4.5 activation at the beginning and end was used to calculate the rundown. This sequence was carried out at SLs: 1.91, 2.05, 2.15 and 2.3 µm for +/+, 2.05, 2.15 ,2.3 and 2.45 µm for +/-, 2.15, 2.3 and 2.50 µm for -/-. Measured stresses at each submaximal activation were normalized by the maximal active stress, and the normalized stresses were plotted against the pCa to determine the tension–pCa curve. Passive stresses were measured just prior to activation. The tension–pCa curves were fit to the Hill equation: T/Tmax (relative tension)= $[Ca^{2+}]^{nH}$ /($K^{+}[Ca^{2+}]^{nH}$), where *n*H is the Hill coefficient, and pCa50=(−logK)/*n*H, pCa for half-maximal activation was calculated. This pCa50 was used as an indicator of Ca^{2+} sensitivity. The pCa_{50}-SL relation of each muscle strip (units pCa/mm sarcomere) was determined and used as an index of the length-dependent activation (i.e. ΔpCa50).

CROSSBRIDGE KINETICS

Three different bathing solutions were used during the experimental protocols: a relaxing solution, a pre-activating solution with low EGTA concentration, and an activating solution. The composition of these solutions was as described previously (33). Fast activation of the fibers was achieved by transferring the skinned fibers from the pre-activation solution containing a low concentration of EGTA (pCa 9.0) to a pCa 4.5 activating solution. Once the steady-state was reached, a slack equivalent to 10% of the muscle length was rapidly induced at one end of the muscle using the motor. This was followed immediately by an unloaded shortening lasting 30 msec. The remaining bound cross-bridges were mechanically detached by rapidly (1 msec) restretching the muscle fiber to its original length, after which tension redevelops. The rate constant of monoexponential tension redevelopment (K_{tr}) was determined by fitting the rise of tension to the following equation: F=Fss(1-e-Ktr.t), where F is force at time t and K_{tr} is the rate constant of tension redevelopment.

To determine force simultaneously with ATP consumption rate, we used the system described by Stienen et al (33). To measure the ATPase activity, a near UV light was projected through the quartz window of the bath (30 µl volume and temperature controlled at 20 ^{0}C) and detected at 340 nm. The maximum activation buffer (pCa 4.5) contained 10 mM phosphoenol pyruvate, with 4 mg/ml pyruvate kinase (500 U/mg^{-}), 0.24 mg ml^{-1} lactate dehydrogenase (870 U/mg) and 20 µM diadenosine-5' pentaphosphate (A2P5). For efficient mixing, the solution in the bath was continuously stirred by means of motor-driven vibration of a membrane positioned at the base of the bath. ATPase activity of the skinned fiber bundles was measured as follows: ATP regeneration from ADP is coupled to the breakdown of phosphoenol pyruvate to pyruvate and ATP catalyzed by pyruvate kinase, which is linked to the synthesis of lactate catalyzed by lactate dehydrogenase. The breakdown of NADH, which is proportional to the amount of ATP consumed, is measured on-line by UV absorbance at 340 nm. The ratio of light intensity at 340 nm (sensitive to NADH concentration) and the light intensity at 410 nm

(reference signal) is obtained by means of an analog divider. After each recording, the UV absorbance signal of NADH was calibrated by multiple rapid injections of 0.25 nmol of ADP (0.025 µl of 10 mM ADP) into the bathing solution, with a stepper motor-controlled injector. The slope of the [ATP] vs. time trace during steady-state tension development of a calcium-induced contraction was determined from a linear fit and the value divided by the fiber volume (in mm^3) to determine the fiber's ATPase rate. ATPase rates were corrected for the basal ATPase measured in relaxing solution. The ATPase rate was divided by tension (force/CSA) to determine the tension cost.

SARCOMERE LENGTH MEASUREMENT OF LEFT VENTRICULAR MID WALL

To determine the SL of the LV at diastasis, we used glutaraldehyde fixation and laser diffraction for SL measurement. Following the PV loop study, KCl/BDM solution was infused through the jugular vein to induce diastolic standstill; when the heart stopped the LV was vented and the hearts were perfusion-fixed with 2% glutaraldehyde through the jugular vein. The hearts were post-fixed and stored in PBS solution. Hearts were cut into 2 mm thick equatorial rings**.** Lateral wall sections of the full wall thickness (approximately 2 mm wide along the circumference) were dissected; thin muscle strips were carefully dissected from the midwall regions for SL measurement. Fiber preparations were placed in a small chamber and SL was measured via laser diffraction with a minimum of 20 fiber measurements averaged per heart.

EXERCISE TESTING

We used 4 month old animals and first allowed animals to undergo voluntary exercise. Individual animals were housed in a large cage that contained a free-running wheel. The exercise wheels have been previously described[34]. Briefly, an 11.5cm diameter wheel with a 5.0cm wide running surface (6208; PetSmart; Phoenix, AZ) was equipped with a digital magnetic counter (BC600, Sigma Sport, Olney Il) that is activated by wheel rotation. After 3 weeks of running, mice were tested for maximal running speed using a 6-lane rodent treadmill system (Exer 3/6, Columbus Instruments, Columbus, OH). After a week acclimation period during which mice were running at low speed, exercise testing was performed by having mice run at progressively increasing speeds (speed steps of 2.5 m/min). Mice ran for 300 sec with a 50 sec rest period between running periods, after which the protocol was repeated but at a 2.5 m/min greater speed. Maximal speed was determined when the mouse left the treadmill and remained on a shock pad for 5 sec. All animals were given water and standard rodent feed ad libitum.

STATISTICS

Statistical analysis was performed in Graphpad Prism (GraphPad Software, Inc). A one-way ANOVA with a Bonferroni post-hoc analysis that calculates *p*-values corrected for multiple comparisons was performed to assess differences between genotypes. When non normally distributed data were analyzed, a Mann-Whitney test was used when comparing two groupsand a Kruskal-Wallis test when comparing three groups, in both cases data were also plotted in dot plots (appended as supplemental Figures). A repeated measure two-way ANOVA with a Tukey's multiple comparison was used to assess differences in

the stress test echocardiographic study and a *t*-test in the exercise study that compared two groups only. Results are shown as mean ± SEM. $p<0.05$ was taken as significant.

Number of cells and mice studied are summarized below:

Figure 1Bi: 114 cells/6 mice +/+, 145 cells/5 mice +/- and 149 cell/7 mice -/-; Figure 1Bii: 71 cells/7 mice +/+, 74 cells/6 mice +/- and 91 cell/8 mice -/-; Figure 1Biii: 20 cells/5 mice +/+, 22 cells/7 mice +/- and 27 cell/7 mice -/-; Figure 1Biv: 138 muscle strips/6 mice +/+, 145 muscle strips/7 mice +/- and 148 muscle strips/7mice -/-.

Figure 2A and Figure 2B top: 12 cells/6 mice +/+, 10 cells/7mice +/- and 15 cells/7mice -/-; Figure 2C, Figure 2B bottom and Figure 2D: 20 cells/5 mice +/+, 22 cells/7 mice +/- and 27 cells/7 mice -/-.

Figure 3A-B: 11 +/+ mice, 12 +/- mice and 10 -/- mice; Figure 3C-D: 9 +/+ mice, 10 +/- mice and 8 -/- mice; Figure 3E-F: 9 +/+ mice, 9 +/- mice and 7 -/- mice; Figure 3G: 6 +/+ mice, 6 +/- mice and 6 -/- mice.

Figure 4B-D: 81 cells/13 mice female +/+, 85 cells/15 mice female +/- and 82 cell/13 mice female -/-.

Figure 5A-C: 12 muscle strips each from 12 mice per group. Figure 5D-F: 11 strips from 11 mice per group.

Figure 6A-B: 12 +/+ mice, 12 +/- mice and 13 -/- mice; Figure 6C-D: 13 +/+ mice, 12 +/- mice and 12 -/- mice.

Figure 7B: 5 C +/+ mice and 5 C+/- mice; Figure 7C: 7 C +/+ mice and 6 C+/- mice; Figure 7D: 7 C +/+ mice and 6 C+/- mice.

Figure S1D: 4 +/+ mice, 4 +/- mice and 4 -/- mice.

Figure S1E: 7 +/+ mice, 7 +/- mice and 9 -/- mice; Figure S1F-G: 1 +/+ mouse, 1 +/- mouse and 1 -/- mouse.

Figure S2a: 3 +/+ mice, 3 +/- mice and 3 -/- mice; Figure S2b: 3+/+ rats, 3-/- rats, 3 +/+ mice, 3 +/- mice and 3 -/- mice.

Figure S2c A: 7 +/+ mice, 7 +/- mice and 7 -/- mice; Figure S2c B: 4 +/+ mice, 4+/- mice and 4 -/- mice; Figure S2c C: 6+/+ mice, 7+/- mice and 10 -/- mice; Figure S2c D: 8+/+ mice, 8+/- mice and 8 -/- mice.

Figure S3A and B: 7 +/+ mice, 7 +/- mice and 7 -/- mice.

Figure S4a A and B: 6 +/+ mice, 5 +/- mice and 5 -/- mice; Figure S4a C: 5 +/+ mice, 5 +/- mice and 5 -/- mice; Figure S4b: 6 +/+ mice, 5 +/- mice and 5 -/- mice; Figure S4c: 7 +/+ mice, 6 +/- mice and 8 -/- mice; Figure S4d: 10 +/+ mice, 10 +/- mice and 9 -/- mice.

Figure S5: 7 cells/1 mouse +/+, 14 cells/ 3 mice +/- and 19 cells /5 mice -/-; Figure S6C: 3 +/+ mice, 3 +/- mice and 3 -/- mice.

Figure S6D: 4 +/+ mice, 4 +/- mice and 4 -/- mice.

Table 1: 13 +/+, 14 +/- and 25 -/- mice and 15 +/+, 14 +/- and 15 -/- mice;

Table S1a: 8 +/+, 12 +/- and 7 -/- mice; Table S1b: 10 +/+, 13 +/- and 7 mice -/-; Table S1c: 13 +/+, 12 +/- and 12 mice -/-.

Table S1d-e: 6 C+/+ and 7 C+/- mice; Table S2a: 10 +/+, 16 +/- and 12 -/- male mice and 9 +/+, 14 +/- and 10 -/-female mice.

Table S2b: 10 +/+, 11 +/- and 8 -/- mice; Table S2c: 6 C +/+ and 7 C+/- mice.

Table S3: 11 +/+mice, 12 +/- mice and 10 -/- mice; Table S4: 81cells/13 mice +/+, 85 cells/15 mice +/- and 82cells/13 mice -/- female mice.

Table S5: please see Figure 5.

To Follow: Supplemental Tables S1-5

Echocardiography	+/+ (n=8)	+/- (n=12)	-/- (n=7)
Age (days)	606.9±13.1	608.8±10.8	626.4±11.7
BW (g)	37.6±3.7	39.9±2.5	36.0±2.5
HR (BPM)	485±13	476±19	472±11
LV-M mode protocol:			
LVID;d (mm)	4.05±0.17	4.18±0.11	4.25±0.11
WT;d (mm)	0.75±0.07	0.77±0.04	0.88±0.06
LVID;s (mm)	2.97±0.15	3.27±0.10	3.27±0.13
WT; s (mm)	0.99±0.07	0.97±0.04	1.09±0.07
Eccentricity	5.82±0.68	5.55±0.32	5.02±0.40
LA (mm)	2.57±0.24	2.51±0.14	2.35±0.18
LV Vol;d (ul)	73.6±7.0	78.4±4.5	81.4±4.9
LV Vol;s (ul)	35.3±4.2	43.9±2.9	43.8±4.2
EF (%)	52.7±2.0	44.2±1.9	46.5±3.5
FS (%)	26.8±1.2	21.8±1.1	23.2±2.2

Table S1a. Echocardiography of LV systolic function of ~20 months old anesthetized female *Rbm20*$^{\Delta RRM}$ mice. Abbreviations: BW: body weight; HR: heart rate; BPM: beats per minute; LV: left ventricle; LVIDd: left ventricular internal diastolic diameter; WTd: diastolic wall thickness; LVIDs; left ventricular internal systolic diameter; WTs: systolic wall thickness; Eccentricity: LVIDd/WTd; LA: left atrium; LV Vold: left ventricular diastolic volume; LV Vols: left ventricular systolic volume; EF: ejection fraction; FS: fractional shortening.

Tail cuff blood pressure measurement			
	+/+ (n=10)	+/- (n=13)	-/- (n=7)
Age (days)	122.8±0.6	127.6±2.4	122.4±2.2
Systolic BP (mmHg)	131.9±6.7	130.1±4.0	129.3±5.1
Diastolic BP (mmHg)	102.0±3.5	106.9±3.8	103.0±6.5
Mean arterial pressure (mmHg)	111.6±4.3	114.4±3.5	111.4±5.8
Pulse rate (beat/min)	589.2±23.5	633.9±15.3	591.0±29.7

Table S1b. Tail cuff blood pressure measurement in conscious male *Rbm20$^{\Delta RRM}$* mice. None of the measured parameters are significantly different.

Conscious echocardiography	Male +/+ (n=13)	+/- (n=12)	-/- (n=12)
Age (days)	137+/-8	140+/-6	132+/-6
BW (g)	27.8+/-1	27.2+/-0.8	26.3+/-0.7
HR (BPM)	635+/-19	669+/-14	633+/-17
LV-M mode protocol:			
LVID;d (mm)	3.63+/-0.09	3.53+/-0.07	3.57+/-0.11
WT;d (mm)	0.9+/-0.02	0.94+/-0.02	0.92+/-0.03
LVID;s (mm)	1.9+/-0.09	1.94+/-0.12	2.23+/-0.15
WT; s (mm)	1.47+/-0.03	1.45+/-0.04	1.35+/-0.04
Eccentricity	4.1+/-0.16	3.77+/-0.1	3.95+/-0.2
LV Vol;d (ul)	56.36+/-3.4	52.16+/-2.54	54.36+/-4.16
LV Vol;s (ul)	11.74+/-1.33	12.69+/-2.05	18.36+/-3.47
FS (%)	47.84+/-1.54	47.48+/-2.45	38.04+/-2.41**,#
SV (μl)	44.61+/-2.39	39.48+/-1.24	36+/-1.82**

Table S1c. Conscious mouse echocardiography of ~ 4 months old male *Rbm20$^{\Delta RRM}$* mice. Conscious M-mode echos were obtained in restrained mice using a parasternal short-axis view at the level of the papillary muscles. Abbreviations: BW: body weight; HR: heart rate; BPM: beats per minute; LV: left ventricle; LVIDd: left ventricular internal diastolic diameter; WTd: diastolic wall thickness; LVIDs; left ventricular internal systolic diameter; WTs: systolic wall thickness; Eccentricity: LVIDd/WTd; LV Vold: left ventricular diastolic volume; LV Vols: left ventricular systolic volume; FS: fractional shortening.; SV: stroke volume. **$p<0.01$ vs WT (+/+); # $p<0.05$ vs het (+/-).

Echocardiography	C+/+ (n=6)	C+/- (n=7)
Age (days)	164.5±7.1	174.7±5.4
BW (g)	30.5±2.9	29.1±1.4
LV-M mode protocol:		
LVID;d (mm)	4.17±0.11	4.23±0.10
WT;d (mm)	0.82±0.03	0.80±0.02
LVID;s (mm)	2.70±0.18	3.05±0.16
WT; s (mm)	1.30±0.12	1.16±0.04
Eccentricity	5.13±0.22	5.32±0.20
LA (mm)	2.64±0.16	2.54±0.05
LV Vol;d (μl)	77.52±4.91	80.41±4.24
LV Vol;s (μl)	27.95±4.40	37.34±4.61
SV(μl)	49.57±6.19	43.07±1.91
FS (%)	35.14±4.43	28.29±2.47
MV decel time (msec)	25.84±0.95	30.94±1.05*

Table S1d. Echocardiography of ~6 months old anesthetized male *α-MHC-Cre; cRbm20$^{\Delta RRM\ flox/+}$* mice. Abbreviations: C+/+: WT; C+/-: one allele with floxed RRM and one allele WT; BW: body weight; LV: left ventricle; LVIDd: left ventricular internal diastolic diameter; WTd: diastolic wall thickness; LVIDs; left ventricular internal systolic diameter; WTs: systolic wall thickness; Eccentricity: LVIDd/WTd; LA: left atrium; LV Vold: left ventricular diastolic volume; LV Vols: left ventricular systolic volume; EF: ejection fraction; FS: fractional shortening.; SV: stroke volume. MV decal time: mitral valve E-wave deceleration time . * $p<0.05$ vs WT (+/+).

Conscious echocardiography	C+/+ (n=6)	C+/- (n=7)
Age (days)	164.5±7.1	174.7±5.4
BW (g)	30.5±2.9	29.1±1.4
HR (BPM)	570.2±10.9	582.0±18.0
LV-M mode protocol:		
LVID;d (mm)	3.85±0.09	3.93±0.12
WT;d (mm)	0.85±0.03	0.90±0.02
LVID;s (mm)	2.34±0.09	2.37±0.12
WT; s (mm)	1.37±0.04	1.37±0.03
Eccentricity	4.56±0.19	4.38±0.14
LV Vol;d (μl)	64.37±3.68	67.70±4.78
LV Vol;s (μl)	19.23±1.80	20.07±2.63
FS (%)	39.25±1.97	39.77±1.86
SV (μl)	45.14±2.89	47.63±3.41

Table S1e. Conscious echocardiography of ~6 months old male *α-MHC-Cre; cRbm20$^{\Delta RRMflox/+}$* mice. Conscious M-mode echos were obtained in restrained mice using a parasternal short-axis view at the level of the papillary muscles. Abbreviations: C+/+: WT; C+/-: one allele with floxed RRM and one allele WT; BW: body weight; HR: heart rate; BPM: beats per minute; LV: left ventricle; LVIDd: left ventricular internal diastolic diameter; WTd: diastolic wall thickness; LVIDs; left ventricular internal systolic diameter; WTs: systolic wall thickness; Eccentricity: LVIDd/WTd; LV Vold: left ventricular diastolic volume; LV Vols: left ventricular systolic volume; FS: fractional shortening.; SV: stroke volume.

Morphometry	Male			Female		
	+/+ (n=10)	+/- (n=16)	-/- (n=12)	+/+ (n=9)	+/- (n=14)	-/- (n=10)
Age (days)	124.3±2.9	124.4±2.6	127.7±3.5	141.8±3.3	140.0±2.9	142.6±1.8
BW (g)	30.7±1.2	28.2±0.8	28.1±0.8	25.3±1.5	20.7±0.6**	21.3±0.7
TL	18.2±0.3	18.2±0.1	18.3±0.1	17.5±0.2	17.0±0.2	17.2±0.2
HW (mg)	141.3±7.0	140.2±4.8	137.4±5.7	105.3±3.5	93.7±3.7*	90.6±2.6**
LV(mg)	93.8±3.1	94.4±2.7	84.0±5.0	73.9±1.9	63.4±2.5*	61.0±1.8**
RV (mg)	23.7±0.9	28.0±1.1	21.8±0.9	21.5±1.1	18.4±0.9	17.9±0.8
ATR (mg)	8.6±0.7	7.8±0.3	8.1±0.5	5.3±0.35	5.5±0.5	5.7±0.3
HW/BW (mg/g)	4.65±0.27	5.03±0.22	4.89±0.14	4.23±0.19	4.52±0.11	4.28±0.16
LV/BW (mg/g)	3.08±0.10	3.38±0.11	2.98±0.15	2.97±0.11	3.06±0.08	2.88±0.11
RV/BW (mg/g)	0.79±0.05	1.00±0.04	0.78±0.03	0.86±0.05	0.89±0.04	0.85.±0.05
ATR/BW(mg/g)	0.28±0.01	0.28±0.01	0.29±0.02	0.21±0.01	0.27±0.02	0.27±0.01
HW/TL (mg/mm)	7.88±0.39	7.69±0.25	7.50±0.29	6.05±0.22	5.49±0.19	5.28±0.14**
LV/TL (mg/mm)	5.16±0.18	5.18±0.14	4.58±0.26	4.25±0.01	3.71±0.12	3.56±0.10*
RV/TL (mg/mm)	1.31±0.05	1.53±0.06	1.19±0.05	1.24±0.01	1.08±0.05	1.04±0.04
ATR/TL (mg/mm)	0.48±0.04	0.43±0.02	0.44±0.03	0.30±0.01	0.32±0.02	0.33±0.01
* significant vs +/+;						

Table S2a. Tissue morphometric study of ~4 months old male and female *Rbm20$^{\Delta RRM}$* mice. BW: body weight; HW: whole heart weight; LV: left ventricle; RV: right ventricle; ATR: weight of left and right atria; TL: tibial length.

Morphometry	+/+ (n=10)	+/- (n=11)	-/- (n=8)
Age (days)	685±24	701±21	670±24
BW (g)	37.8±3.1	41.2±2.6	35.4±2.4
TL (Tibial length)	19.1±0.2	19.3±0.2	18.8±0.2
HW (mg)	150.7±8.0	153.0±4.3	150.1±6.7
LV(mg)	102.2±6.0	100.6±4.1	100.8±4.8
RV (mg)	30.9±1.7	31.2±1.2	27.6±2.4
L ATR (mg)	3.8±0.3	4.9±0.3	5.1±0.4
R ATR (mg)	5.3±0.4	5.8±0.5	6.4±0.6
HW/BW (mg/g)	4.12±0.23	3.82±0.20	4.41±0.43
LV/BW (mg/g)	2.78±0.15	2.51±0.14	2.97±0.31
RV/BW (mg/g)	0.85±0.05	0.78±0.05	0.78±0.04
L ATR/BW(mg/g)	0.11±0.01	0.12±0.01	0.14±0.01
R ATR/BW (mg/g)	0.14±0.01	0.14±0.02	0.18±0.02
HW/TL (mg/mm)	7.92±0.45	7.94±0.25	7.97±0.31
LV/TL (mg/mm)	5.37±0.34	5.22±0.23	5.35±0.22
RV/TL (mg/mm)	1.62±0.09	1.62±0.07	1.47±0.12
L ATR/TL (mg/mm)	0.20±0.01	0.25±0.02	0.27±0.02
R ATR/TL (mg/mm)	0.28±0.02	0.30±0.02	0.34±0.03
LUNG/BW(mg/g)	5.0±0.3	5.3±0.6	5.3±0.6
LIVER/BW(mg/g)	40.0±1.8	35.8±1.8	40.0±1.8
LUNG/TL (mg/mm)	9.5±0.4	10.7±0.9	9.5±0.5
LIVER/TL (mg/mm)	78.5±7.8	76.4±5.8	74.0±3.1

Table S2b. Tissue morphometric study of ~20 months old female *Rbm20$^{\Delta RRM}$* mice. BW: body weight; HW: whole heart weight; LV: left ventricle; RV: right ventricle; ATR: atria. TL: tibia length

Morphometry	C+/+ (n=6)	C+/- (n=7)
Age (days)	164.5±7.1	174.7±5.4
BW (g)	30.5±2.9	29.1±1.4
TL	18.2±0.2	18.0±0.1
LV(mg)	100.2±3.9	104.7±4.5
RV (mg)	27.7±0.5	27.5±1.9
L ATR (mg)	4.6±0.3	5.0±0.4
R ATR (mg)	4.9±0.4	4.4±0.3
LV/BW (mg/g)	3.37±0.19	3.63±0.20
RV/BW (mg/g)	0.94±0.08	0.96±0.08
L ATR/BW(mg/g)	0.16±0.01	0.17±0.01
R ATR/BW (mg/g)	0.16±0.00	0.15±0.01
LV/TL (mg/mm)	5.52±0.20	5.82±0.26
RV/TL (mg/mm)	1.53±0.04	1.53±0.11
L ATR/TL (mg/mm)	0.25±0.02	0.28±0.02
R ATR/TL (mg/mm)	0.27±0.02	0.25±0.02
LUNG/BW(mg/g)	5.02±0.30	4.94±0.20
LUNG/TL (mg/mm)	8.22±0.36	7.97±0.40

Table S2c. Tissue morphometric study of ~6 months old male *α-MHC-Cre; cRbm20$^{\Delta RRMflox/+}$* mice. BW: body weight; HW: whole heart weight; LV: left ventricle; RV: right ventricle; ATR: atria; TL: tibial length. No significant changes were found in C+/- mice.

Pressure-Volume Analysis	Male +/+ (n=11)	+/- (n=12)	-/- (n=10)
Load Dependent Parameters			
HR (bpm)	540+/-13	525+/-14	514+/-10
ESP (mmHg)	91+/-3	97+/-3	71+/-2****####
EDP (mmHg)	6+/-1	7+/-1	5+/-1
dPmax (mmHg/s)	8494+/-349	8751+/-576	7505+/-337
dPmin (mmHg/s)	-8113+/-389	-8133+/-596	-6225+/-305**##
ESV (µl)	33+/-2	36+/-3	40+/-2
EDV (µl)	65+/-3	67+/-5	71+/-3
SV (µl)	32+/-2	31+/-2	31+/-1
EF (%)	49+/-2	46+/-2	44+/-1*
Tau Glantz (ms)	9.6+/-1.3	9.5+/-0.8	9.8+/-0.8
Ea (mmHg/µl)	3+/-0.2	3.2+/-0.2	2.4+/-0.1*##
Load Independent Parameters			
Ees (mmHg/µl)	3.8 +/- 0.1	2.7+/-0.3***	1.9+/-0.2****####
V0 (µl)	7+/-2.3	-1.6+/-4.6	-6+/-5.5
EDPVR (mmHg/µl)	0.046+/-0.003	0.02+/-0.003****	0.024+/-0.002****

Table S3. Pressure (P)-volume (V) analysis in male *Rbm20*$^{\Delta RRM}$ mice. PV analysis was performed on lightly anesthetized and ventilated 4 months old using %1.5 isoflurane. Body temperature was maintained at 37 °C and a 1.2F PV catheter was introduced retrograde into the LV through the left carotid artery. All measurements were obtained during a pause in ventilation. Inferior venal caval occlusions were performed to assess load-independent parameters. Abbreviations: see caption for Tables S1-S3; Additionally, ESP: end-systolic pressure; EDP: end-diastolic pressure; ESV: end-systolic volume; EDV: end-diastolic volume; EF: ejection fraction; Ea: effective arterial elastance; Ees: end-systolic elastance; V0: volume at which there is 0mmHg pressure in the left ventricle. This is the x-axis intercept of the linear fit of the end-systolic elastance (Ees). EDPVR: end-diastolic PV relationship. Symbols:*p<0.05, **p<0.01, ***p<0.001, ****p<0.0001 vs. wild-type (+/+); ##p<0.01, ####p<0.0001 vs. Het (+/-).

Systolic function of intact and skinned cardiocytes			
	+/+	**+/-**	**-/-**
Intact cardiocytes			
number of cells/mice	81/13	85/15	82/13
Systolic stress at baseline[ǂ]	5.1±0.3	4.9±0.3	3.8±0.2**,#
Diastolic SL at baseline (µm)	1.90±0.01	1.95±0.00****	2.00±0.00****,####
Systolic SL at baseline (µm)	1.73±0.01	1.74±0.01	1.78±0.01***,#
Systolic stress vs Systolic SL[ǂǂ]	67.5±4.4	45.7±3.8****	25.5±1.7****,###
Systolic stress vs Diastolic SL[ǂǂ]	24.6±1.1	15.4±0.8****	10.4±0.5****,###
Systolic stress vs Diastolic stress	1.18±0.04	1.20±0.05	1.20±0.04
Skinned cardiocyte			
number of cells/mice	16/8	20/7	16/6
Active stress at pCa 4.5[ǂ]	43.6±5.4	47.3±4.5	31.7±3.0#

[ǂ] mN/mm^2

[ǂǂ] mN/mm^2.µm/SL

Table S4. Systolic function of intact cardiocytes of *Rbm20*$^{\Delta RRM}$ mice. FSM of intact cells was calculated from the slope of the systolic stress-systolic SL relation and systolic stress-diastolic SL relation. Bottom of table shows that maximal active stress of skinned cardiac myocytes (SL 2.0 µm) was reduced in -/- cells (relative to +/+ cells). Symbols: **p<0.001, ***p<0.001, ****p<0.0001 vs. wild-type (+/+); #p<0.05, ###p<0.001, ####p<0.0001 vs. Het (+/-).

	SL	pCa_{50}	LDA	nH	Stress max	Tension cost	Ktr(s^{-1})
+/+	1.91(BL)	5.95±0.01	0.46±0.05	3.07±0.17	41.0±4.2	ND	ND
+/+	2.05	5.99±0.02		2.91±0.12	51.2±2.5	1.86±0.11	25.0±1.93
+/+	2.15	6.02±0.03		2.94±0.03	56.5±3.2	1.77±0.08	25.2±1.30
+/+	2.3	6.11±0.03		2.62±0.06	62.5±2.1	1.48±0.09	25.5±0.90
+/-	2.05(BL)	5.96±0.02	0.26±0.04**	2.90±0.05	44.7±2.3	2.01±0.12	27.7±3.2
+/-	2.15	5.99±0.02		2.78±0.06	51.5±3.9	1.86±0.14	25.2±1.3
+/-	2.30	6.03±0.02*		2.92±0.11	53.4±2.9*	1.68±0.09	24.2±1.2
+/-	2.45	6.05±0.03		2.61±0.15	57.5±1.2	ND	ND
-/-	2.15(BL)	5.95±0.01*#	0.19±0.03**	2.95±0.17	33.3±2.2**##	2.23±0.15*	23.8±1.4
-/-	2.30	5.96±0.01**##		2.94±0.22	38.1±2.3***##	1.98±0.10*#	25.7±1.1
-/-	2.50	5.99±0.01		2.98±0.21	43.3±3.0	1.90±0.10	23.7±1.1

Table S5. Contractility measurements in LV papillary muscle *of Rbm20$^{\Delta RRM}$* mice. * significance vs. -/- at same SL (ANOVA); # significance vs. +/- at same SL (ANOVA). SL: sarcomere length (mm); BL= sarcomere length of slack preparation. LDA: length dependent activation obtained from fitting the pCa_{50}-SL relation of each muscle strip (units pCa/mm sarcomere). Fmax; tension at pCa 4.5 (in mN/mm^2). Tension cost: ATPase rate/tension (in pmol/(mm mN s). ND: not determined. Ktr: rate constant of tension recovery following rapid release-restretch (in s^{-1}). Symbols: *p<0.05, **p<0.01, ***p<0.001 vs. wild-type (+/+); $^{\#}$p<0.05, $^{\#\#}$p<0.01, vs. Het (+/-). *11 muscle strips in each group.*

To Follow: Supplemental Figures S1-11

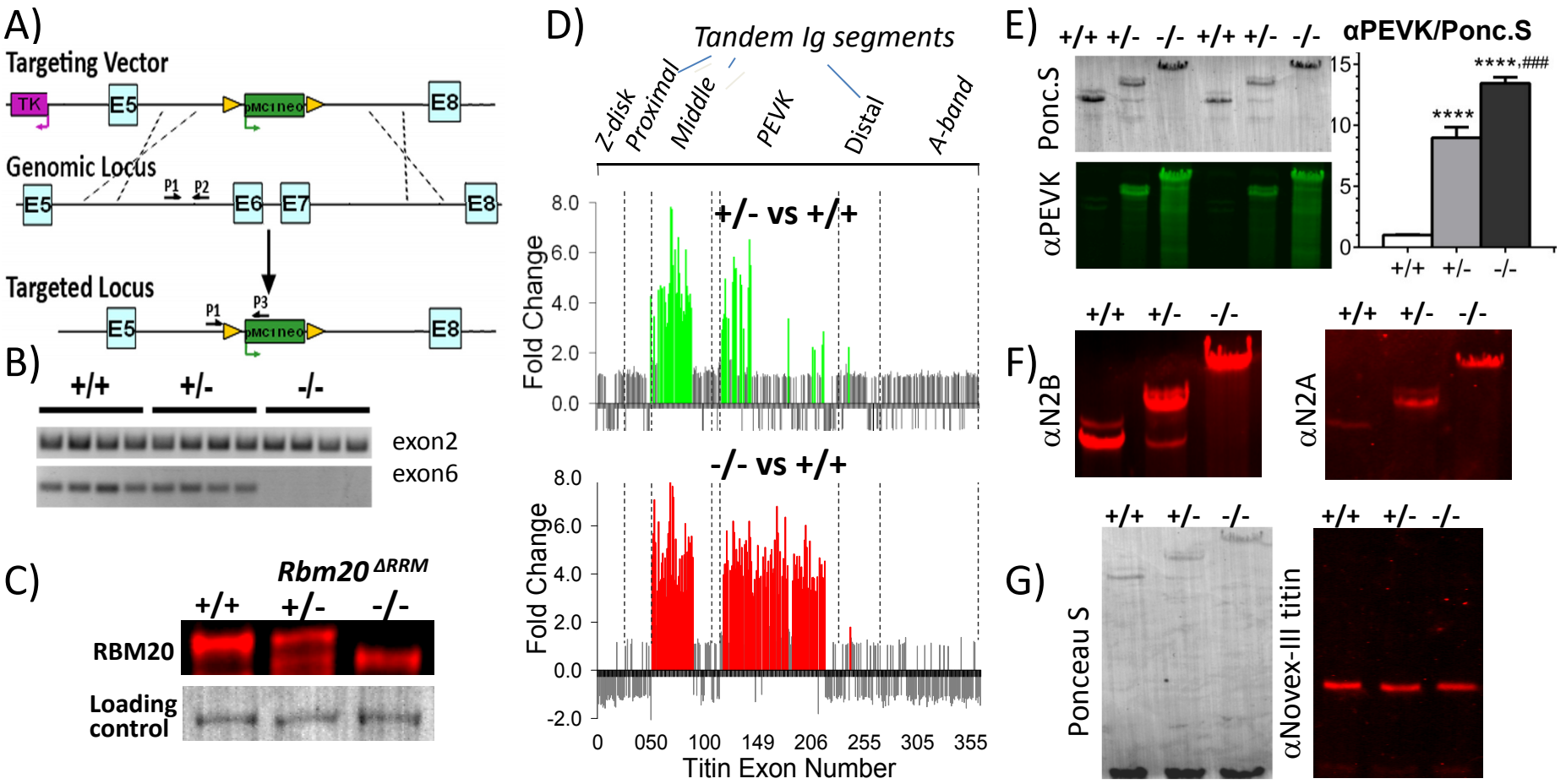

Figure S1. Generation of mice lacking RBM20's RNA Recognition Motif (RRM). A) Targeting vector design resulting in an in-frame deletion of the RRM encoded by exons 6 and 7. Details in Supplemental Methods. B) PCR analysis of expression of RBM20 exon 2 (not deleted) and RBM20 exon 6 (deleted). C) Western blot analysis with an antibody against RBM20's conserved N-terminus (outside the deleted region) shows expected expression patterns of wild-type RBM20 protein and higher mobility mutant RBM20 protein. D) Titin exon microarray analysis in *Rbm20*$^{\Delta RRM}$ LV. Many exons encoding Ig domains are upregulated in both +/- and -/- LV while many more PEVK domains are incorporated in the -/- compared to +/- LV. E-G) Western blots probing titin expression in *Rbm20*$^{\Delta RRM}$ LV. Experiments with the 9D10 antibody that recognizes repeating sequences within the PEVK element confirm upregulation of PEVK exons(E). Antibodies against cardiac titin's N2B spring element (exon 49) and cardiac titin's N2A element (exons 102-19) showed that the large titins expressed in *Rbm20*$^{\Delta RRM}$ mice are of the N2BA type (F). We also studied the Novex-III exon (exon 48) and found that it is not incorporated in the giant titins of the *Rbm20*$^{\Delta RRM}$ mouse (G). Instead the antibody detects the ~700 kDa novex-3 titin (a small titin isoform expressed at low levels[2]) with no differences amongst genotypes, indicating that RBM20 does not control splicing of novex-3 titin. *D: 4 +/+ mice, 4 +/- mice and 4 -/- mice; E: 7 +/+ mice, 7 +/- mice and 9 -/- mice; F-G: 1 +/+ mouse, 1 +/- mouse and 1 -/- mouse.*

Blue outline: titin (Ttn) exons

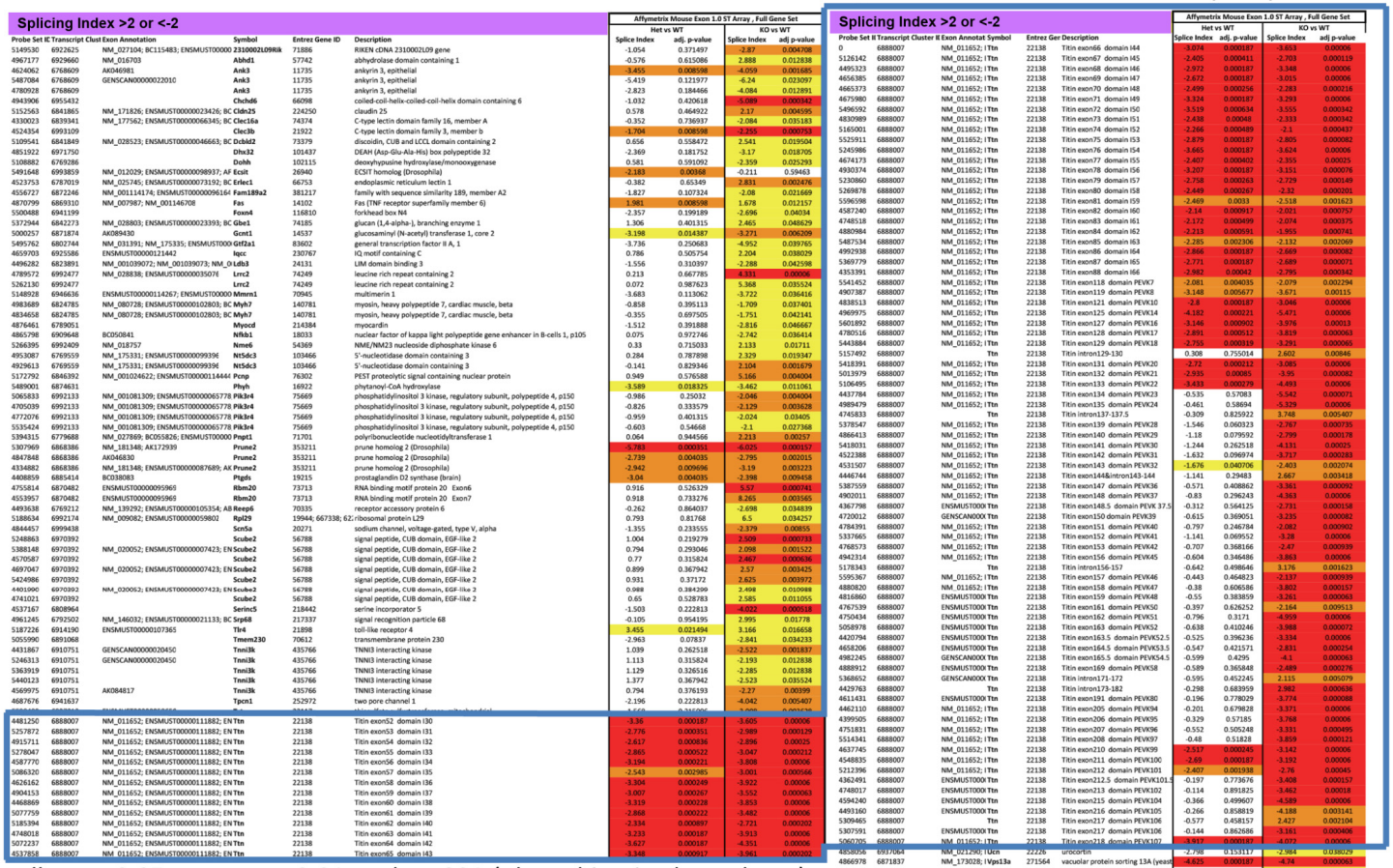

yellow p<0.05, orange p<0.01, red p<.001 (plotted in pie chart above)

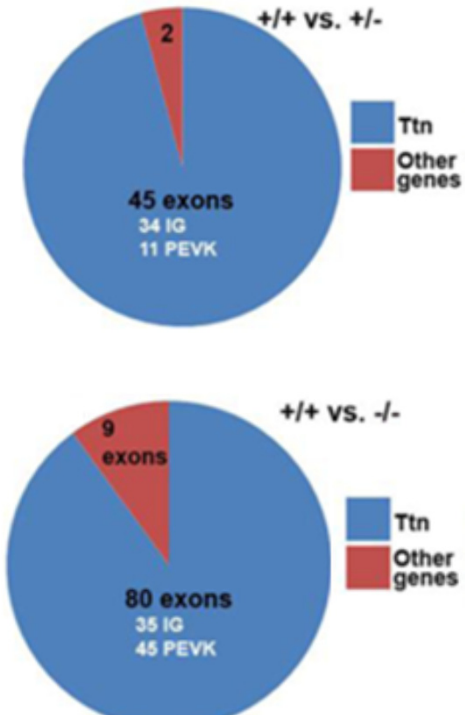

See supplemental Excel spreadsheet for details

Figure S2a. Exon GeneChip microarray results identify titin gene (*Ttn*) as the predominant splicing target affected in left ventricular tissue. Pie charts at top show the distribution of exons affected in +/- (left) or -/- (right) for the *Rbm20*$^{\Delta RRM}$ mutation at the p<0.001 level. This platform confirms the observation with our custom array that exons encoding the Ig domains of titin are more sensitive to RBM20 dose than the PEVK exons; Ig domains 28-67 are incorporated in both +/- and -/- hearts while many more PEVK domains are incorporated in the -/- than+/- hearts. Supplemental Excel spreadsheets provide more details in exon level and gene level changes. There were no changes in gene expression level at p≤0.01. *a: 3 +/+ mice, 3 +/- mice and 3 -/- mice.*

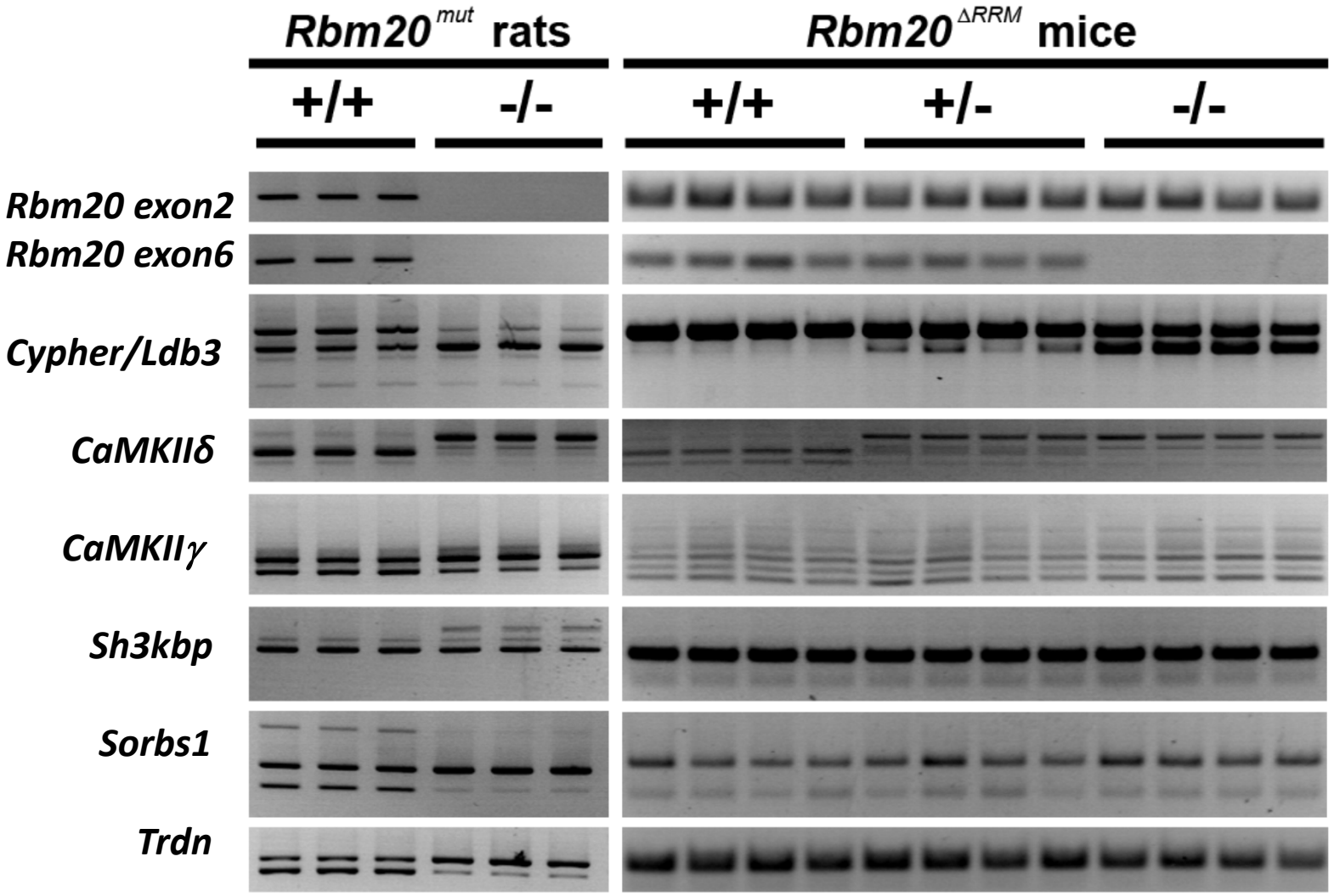

Figure S2b. **Multiple genes that are alternatively spliced in the mutant rat are unaltered in the *Rbm20$^{\Delta RRM}$* mouse.** Endpoint RT-PCR analysis confirms that the spontaneous rat mutation in *Rbm20* resulted in deletion of all but the first exon removing all *Rbm20* function and that the targeted mouse *Rbm20$^{\Delta RRM}$* deletion only removes exons 6-7. RT-PCR comfirms changes in splicing in *Rbm20mut* rats for *Cypher/Ldb3*, *CaMKIIδ*, *CaMKIIγ*, *Sh3kbp*, *Sorbs1* and *Trdn*. In the *Rbm20$^{\Delta RRM}$* -/- mice a similar change in *CaMKIIδ* splicing occurs as seen in *Rbm20mut* rats. Mouse *Cypher/Ldb3* shows a change in isoform ratio in *Rbm20$^{\Delta RRM}$* -/- to make it more similar to what is seen in wild-type rats. The rat RBM20-targets: *CaMKIIγ*, *Sh3kbp*, *Sorbs1* and *Trdn* show no change in splicing in the *Rbm20$^{\Delta RRM}$* mouse model. *b: 3+/+ rats, 3-/- rats, 3 +/+ mice, 3 +/- mice and 3 -/- mice.*

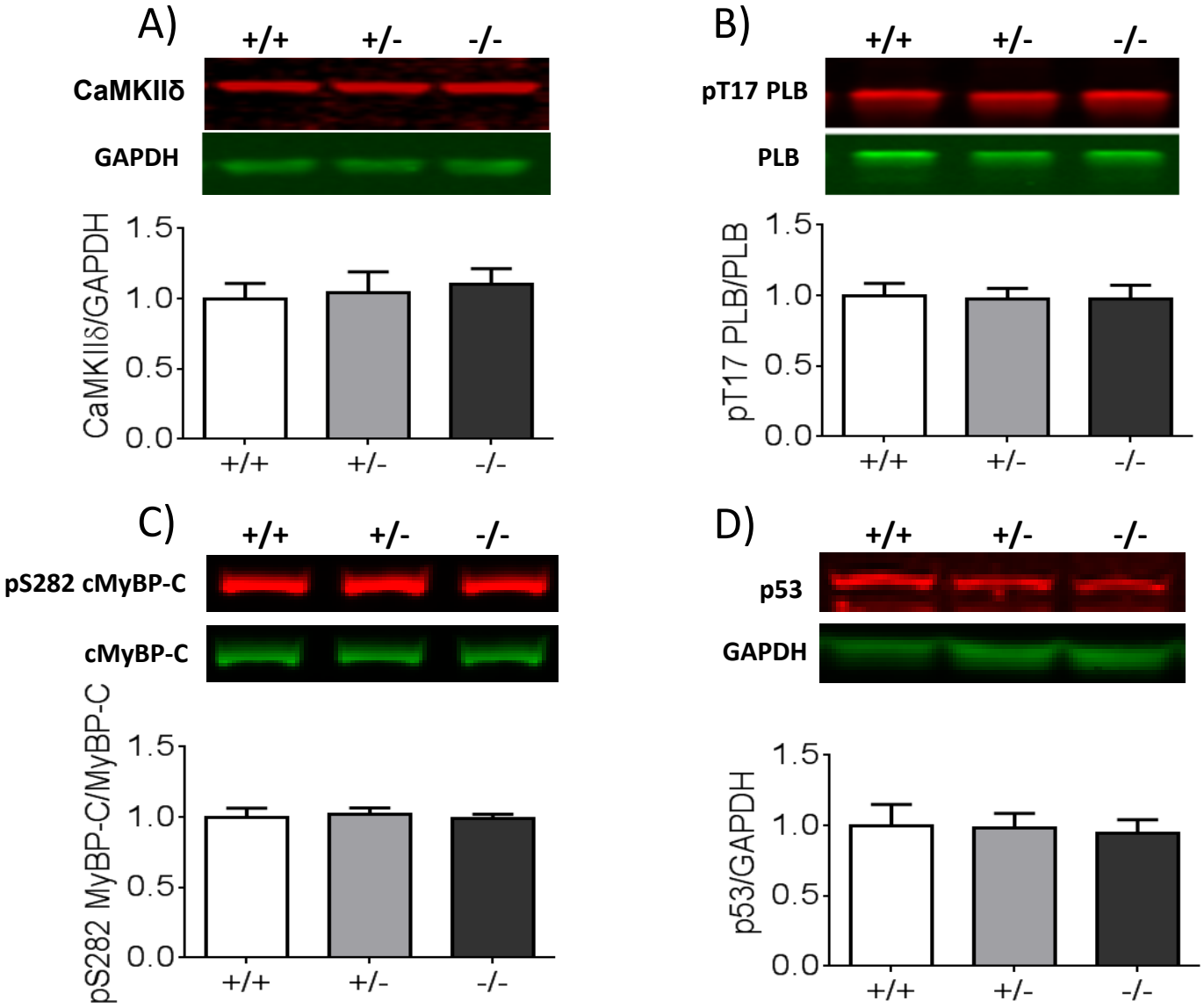

Figure S2c. CaMKIIδ protein levels (A) and analysis of CaMKIIδ downstream targets (B-D) in *Rbm20$^{\Delta RRM}$* mouse model. No changes are found in the protein levels of total CaMKIIδ (A) and its downstream target p53 (D). No changes are found in the phosphorylation levels of the downstream targets T17 of PLB(B) and S282 of cMyBP-C (C). *S2c A: 7 +/+ mice, 7 +/- mice and 7 -/- mice; S2c B: 4 +/+ mice, 4+/- mice and 4 -/- mice; S2c C: 6+/+ mice, 7+/- mice and 10 -/- mice; S2c D: 8+/+ mice, 8+/- mice and 8 -/- mice.*

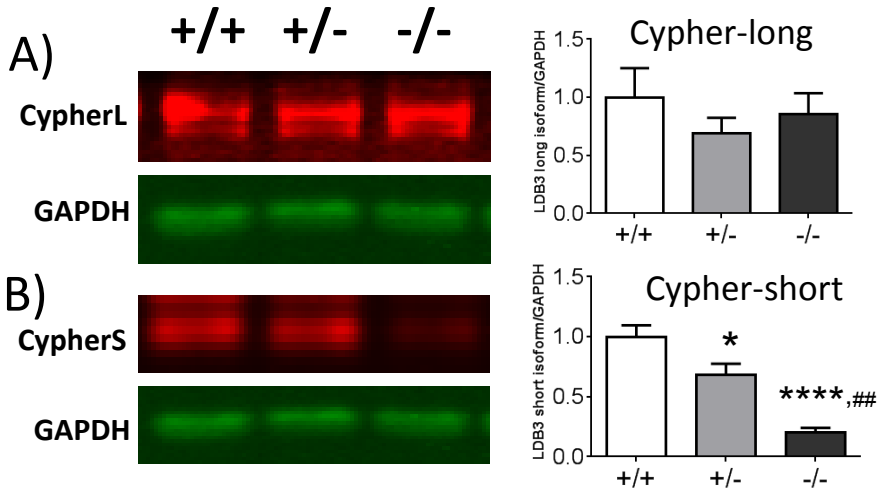

Figure S3. *Cypher* is alternatively spliced in *Rbm20*$^{\Delta RRM}$ mice. A and B) Western blot analysis of long and short cardiac Cypher isoforms reveals a decreased expression of the cardiac short isoform in the hearts of +/- and -/- mice. *S3A and B: 7 +/+ mice, 7 +/- mice and 7 -/- mice.* Symbols: *p<0.05, ****p<0.0001 vs. wild-type (+/+); $^{\#\#}$p<0.01 vs. Het +/-.

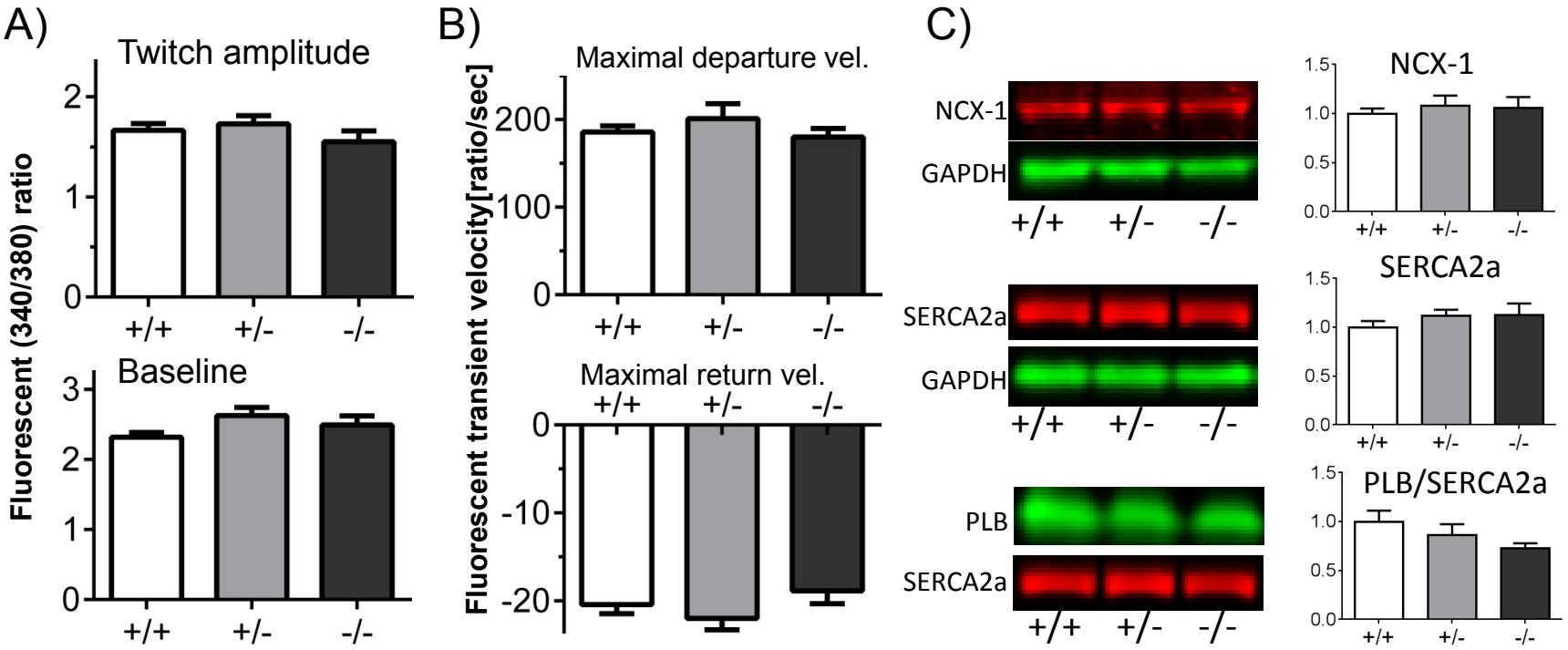

Figure S4a. Ca^{2+} handling of *Rbm20$^{\Delta RRM}$* cardiocytes. A and B) Fura-2 340/380 ratio of isolated intact cardiomyocytes stimulated at 2 Hz. Twitch amplitude and baseline signal (A) as well as maximal velocities of rising and decaying signal (B) are not different. C) Representative western blots of NCX-1, SERCA2a, and PLB (monomeric form) normalized by SERCA2a expression. There are no significant changes. *S4a A and B: 6 +/+ mice, 5 +/- mice and 5 -/- mice; S4a C: 5 +/+ mice, 5 +/- mice and 5 -/- mice.*

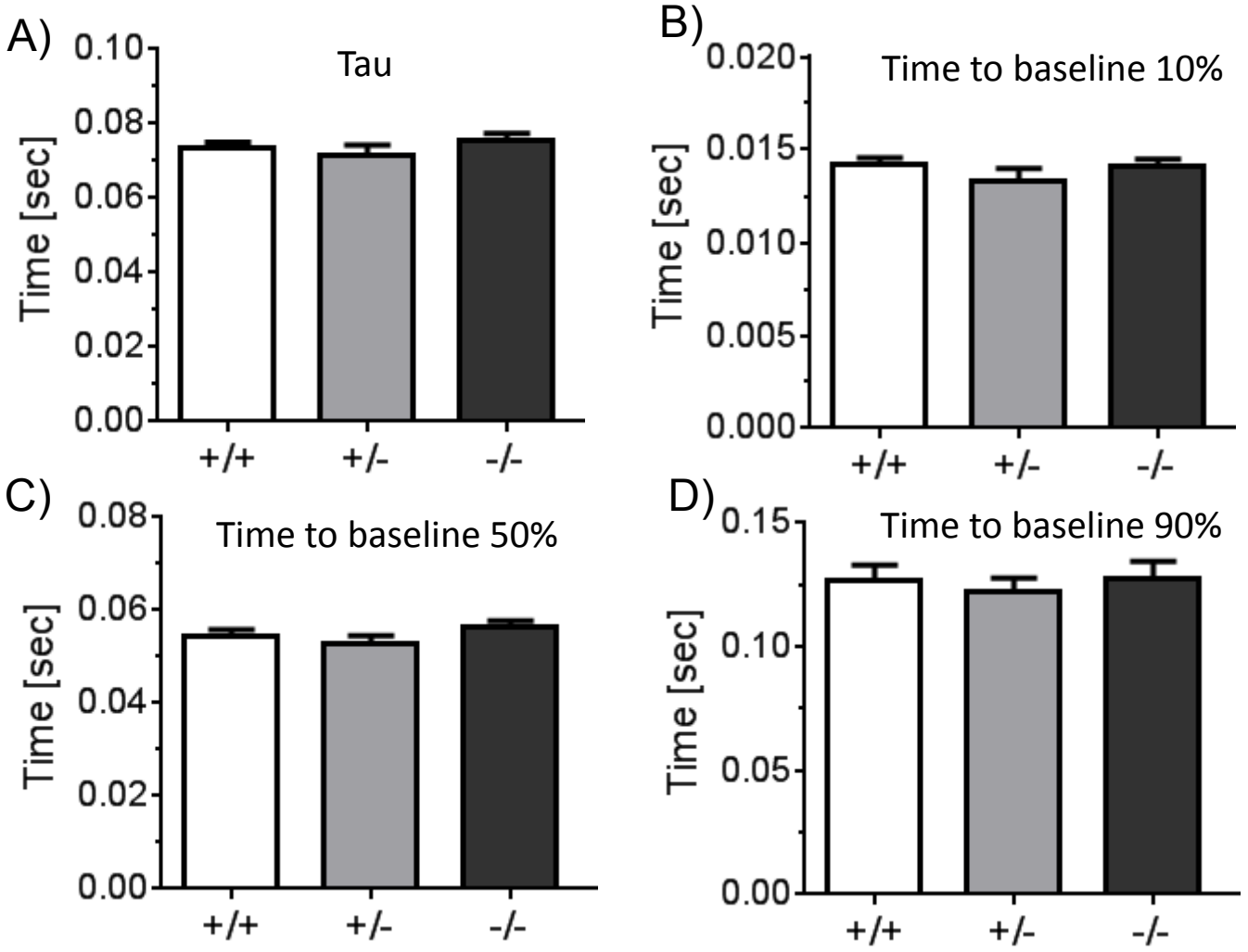

Figure S4b. Ca^{2+} re-uptake parameters of *Rbm20$^{\Delta RRM}$* cardiocytes. Ca^{2+} reuptake determined from transient's return phase of Fura-2 340/380 signal measured from isolated intact cardiomyocytes stimulated at 2 Hz. (A) Exponential decay time constant (Tau), (B, C, and D) time for the transient to return 10% , 50% , and 90% of the peak. There are no significant changes between the genotypes. *Figure S4b: 6 +/+ mice, 5 +/- mice and 5 -/- mice.*

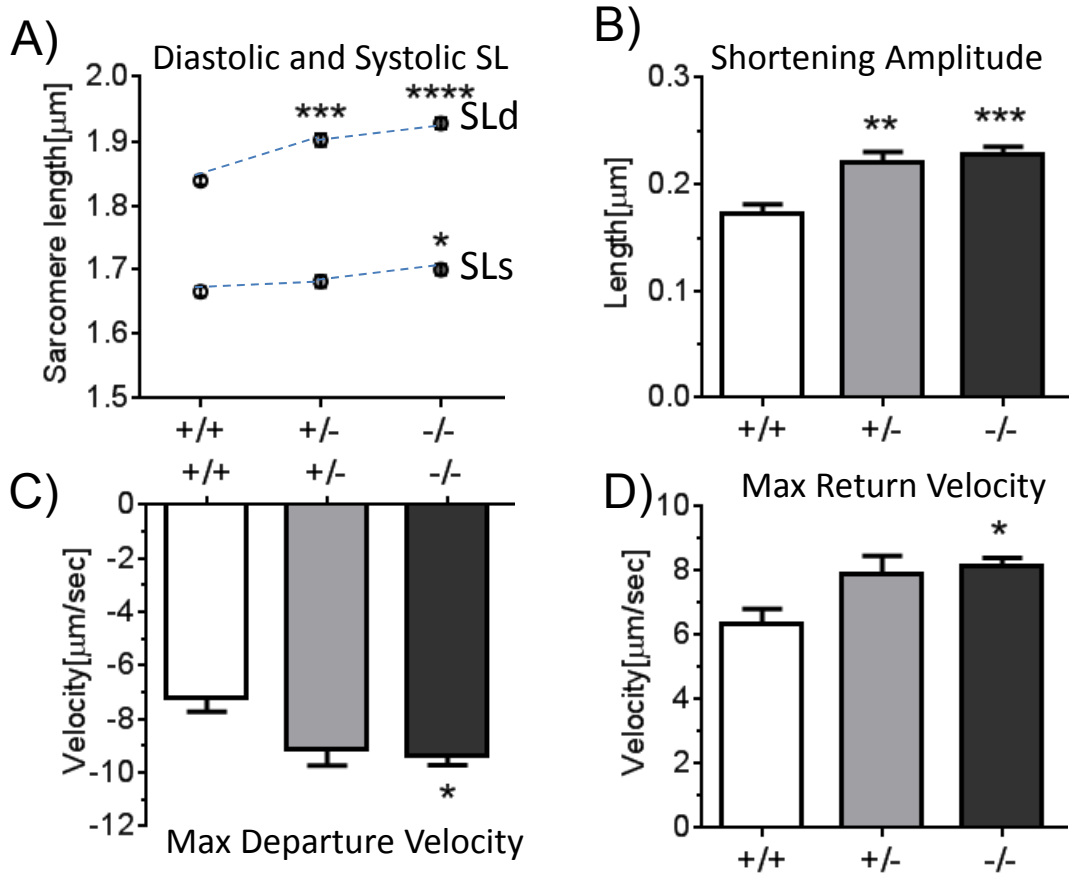

Figure S4c. Shortening of unloaded intact cells beating at 2 Hz. A) End-Diastolic SL (SLd) and End-Systolic SL (SLs) of +/+, +/- and -/- *Rbm20*$^{\Delta RRM}$ cells. B) Shortening amplitude of +/- and -/- cells is larger than of +/+ cells, which is mostly due to their larger SLd. C) and D) Maximal departure and maximal return velocity are higher in -/- mice. *S4c: 7 +/+ mice, 6 +/- mice and 8 -/- mice.* Symbols: *p<0.05, ***p<0.001, ****p<0.0001 vs. wild-type (+/+).

An explanation for the larger shortening amplitude of +/- and -/- *Rbm20*$^{\Delta RRM}$ cells is the titin-based *restoring* force against which unloaded cells have to shorten (this is a negative force that is present below the slack length of cells and that pushes out on the Z-disks). Restoring force scales with the fractional extension of titin's extensible region and for a given sarcomere length below the slack length the restoring force will be less in +/- and -/- cells than in wt cells. Consistent with this is the higher maximal departure velocity of unloaded beating +/- myocytes (Panel C). (The increased maximum return velocity of -/- cells in panel D can not be explained by restoring force differences. Considering that the maximum return velocity is reached while the calcium transient has decayed to only ~ 50% of its peak (results not shown) the increased max return velocity of -/- cells might be due to their lower calcium sensitivity).

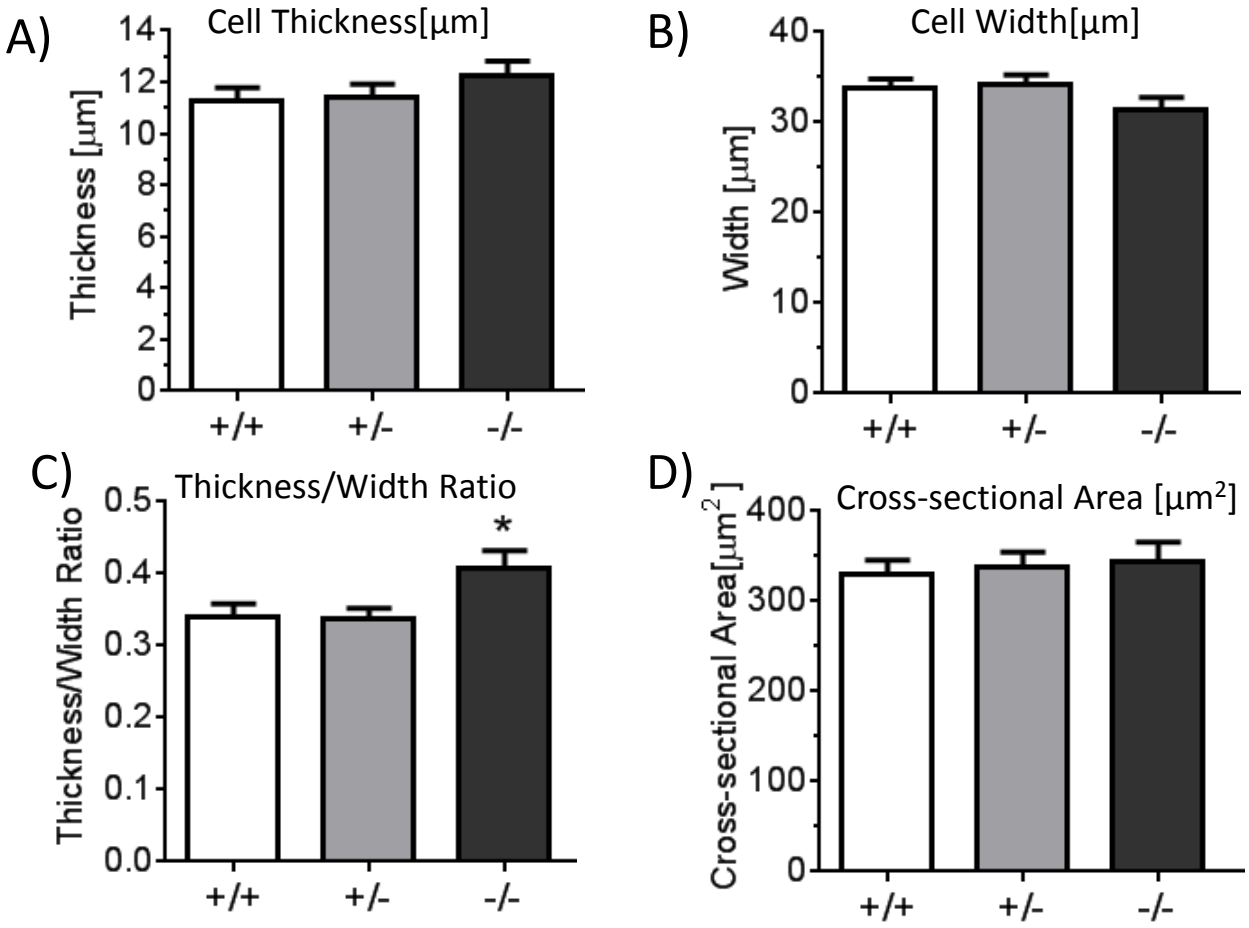

Figure S4d. Cell dimensions of skinned cardiocytes. Cell were imaged perpendicular to their long axis. Thickness /width ratio is significantly increased in -/- cells. Cross-sectional area is unaltered. *S4d: 10 +/+ mice, 10 +/- mice and 9 -/- mice.*

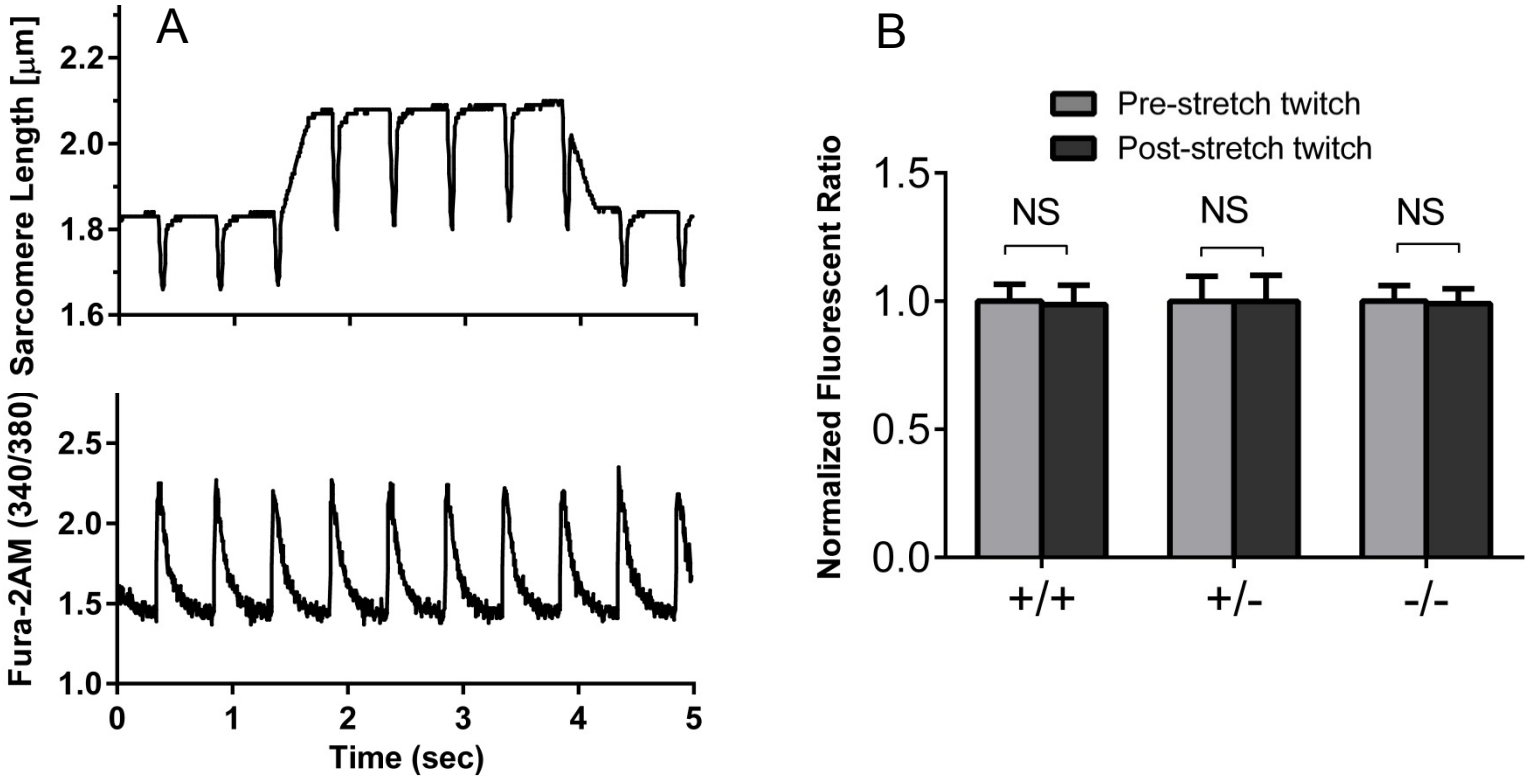

Figure S5. Ca^{2+} transient before and after 10% length change. A) Simultaneous recording of SL and Fura-2 (340/380 ratio) in intact cardiomyocytes. B) Transient amplitudes of the last twitch at baseline (pre-stretch twitch) versus the immediate twitch after 10% stretch (post-stretch twitch) were not different. *7 cells +/+, 14 cells +/- and 19 cells -/-.*

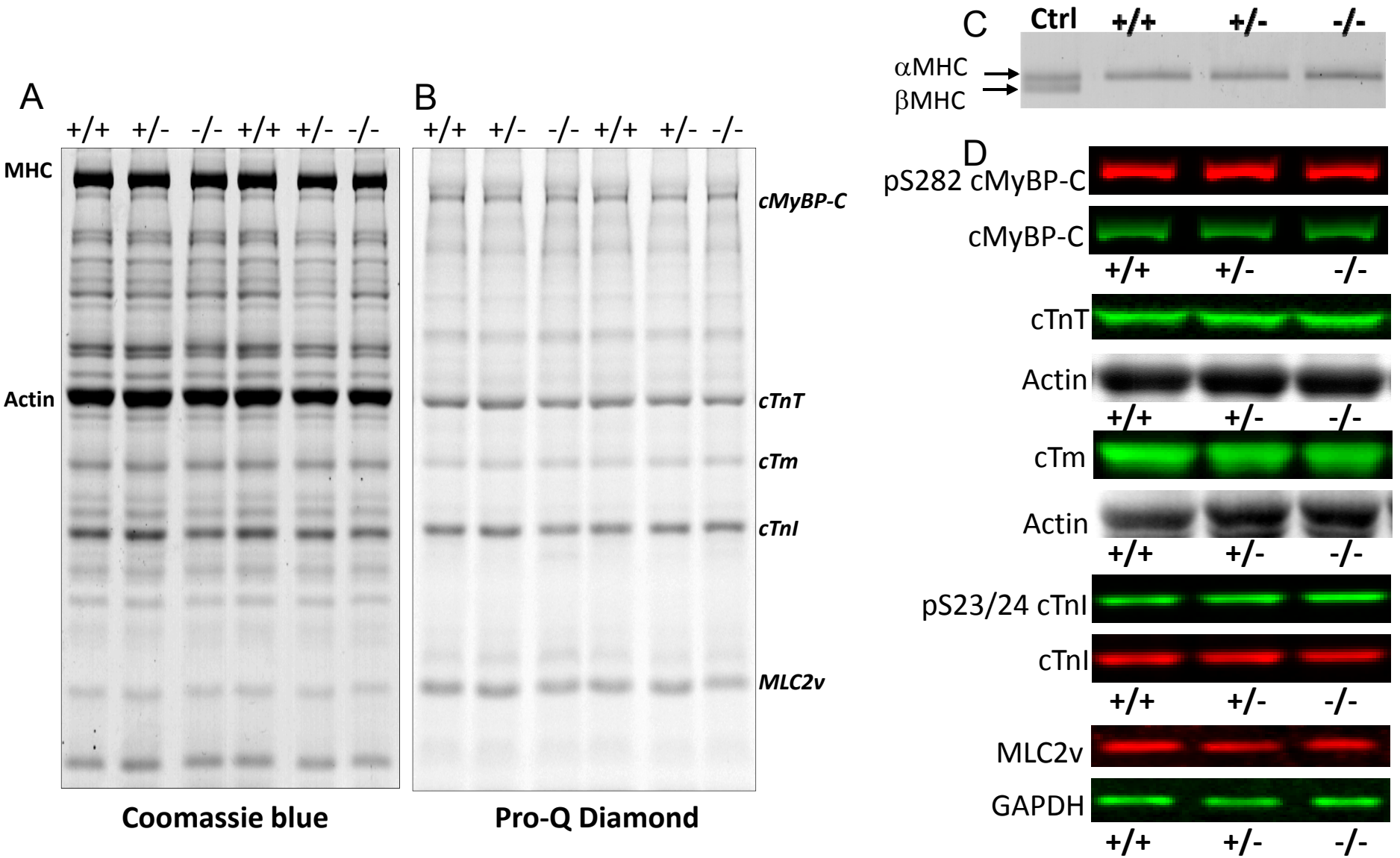

Figure S6. Myofilament protein analysis in LV. A and B) Representative Coommassie blue and Pro-Q Diamond stained gel. There are no noticeable differences in the phosphorylation level of the myofilament proteins amongst the three groups. C) Myosin heavy chain (MHC) expression. A 1-day old neonatal sample (ctrl) is shown for reference as it expresses both α-MHC and β-MHC. There is no detectable change in MHC isoform expression in the three groups. D) Regulatory proteins expression and specific phosphorylation sites. pS282 cMyBP-C was normalized by total cMyBP-C, cTnT, and TM with actin as a loading control; pS23/24 cTnI was normalized by total cTnI and MLC2v with GAPDH as a loading control. There are no significant differences amongst the three groups. *C: 3 +/+ mice, 3 +/- mice and 3 -/- mice; D: 4 +/+ mice, 4 +/- mice and 4 -/- mice.*

In vivo characterization of LV diastolic compliance (from Fig 3)

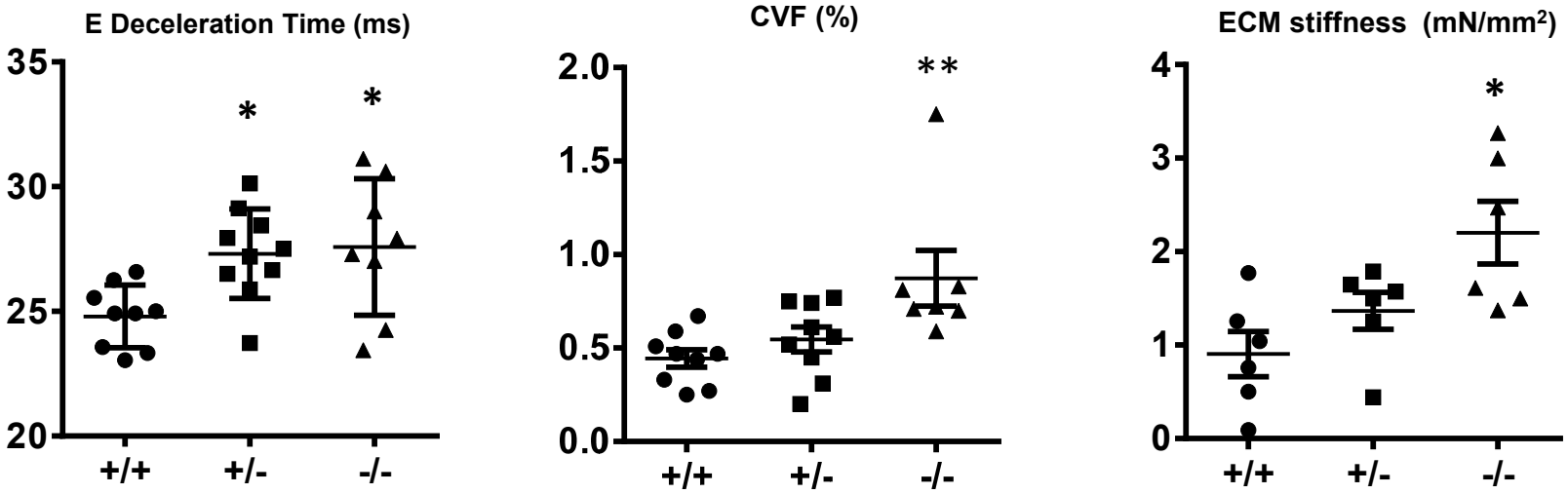

Exercise capacity of C+/- and C+/+ mice (from Fig 7)

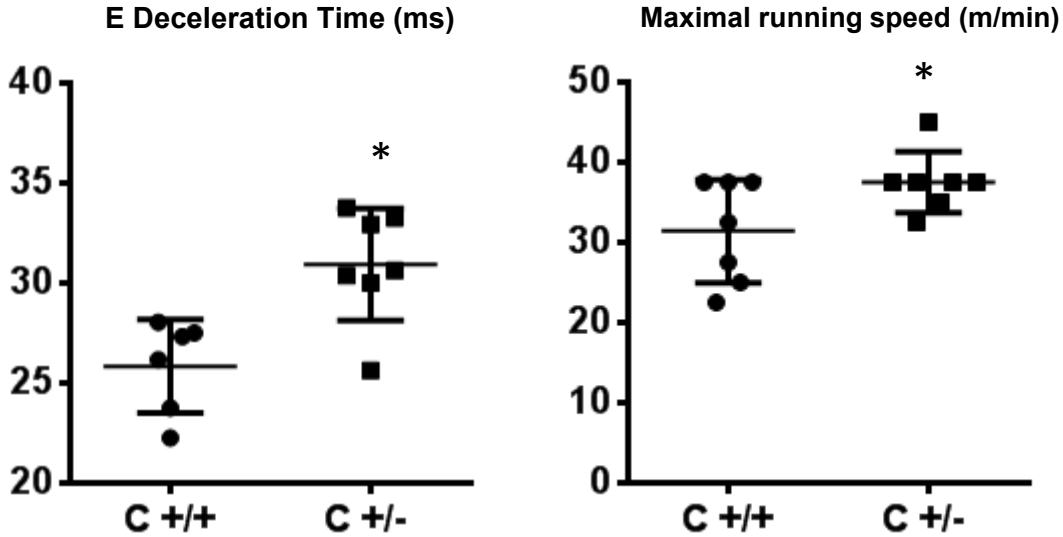

Figure S7

Echocardiography of anesthetized male *α-MHC-Cre; cRbm20$^{\Delta RRM}$* mice (from Table S1d)

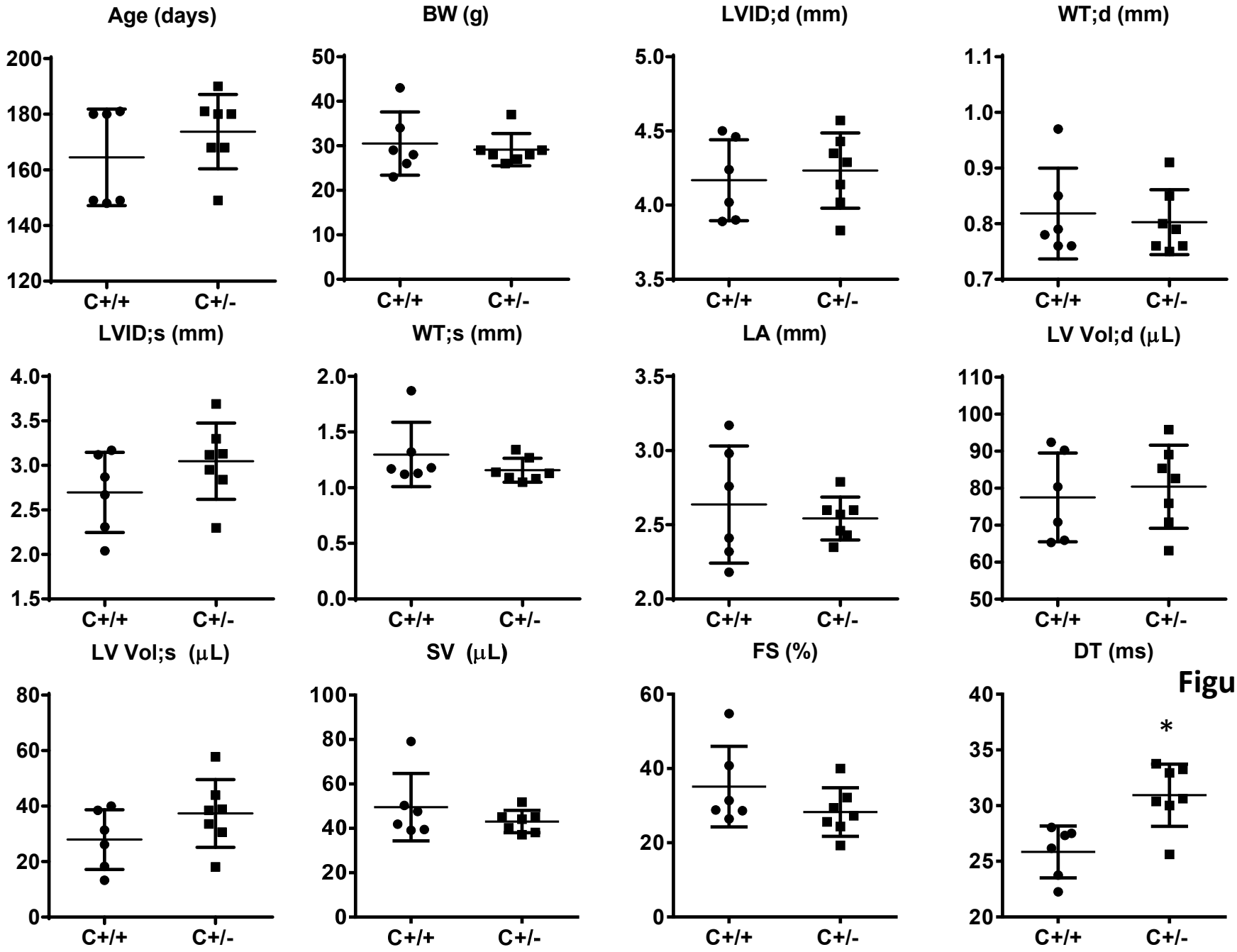

Figure S8

Echocardiography of ~6mo old conscious male *α-MHC-Cre; cRbm20$^{\Delta RRM}$* mice (from Table S1e)

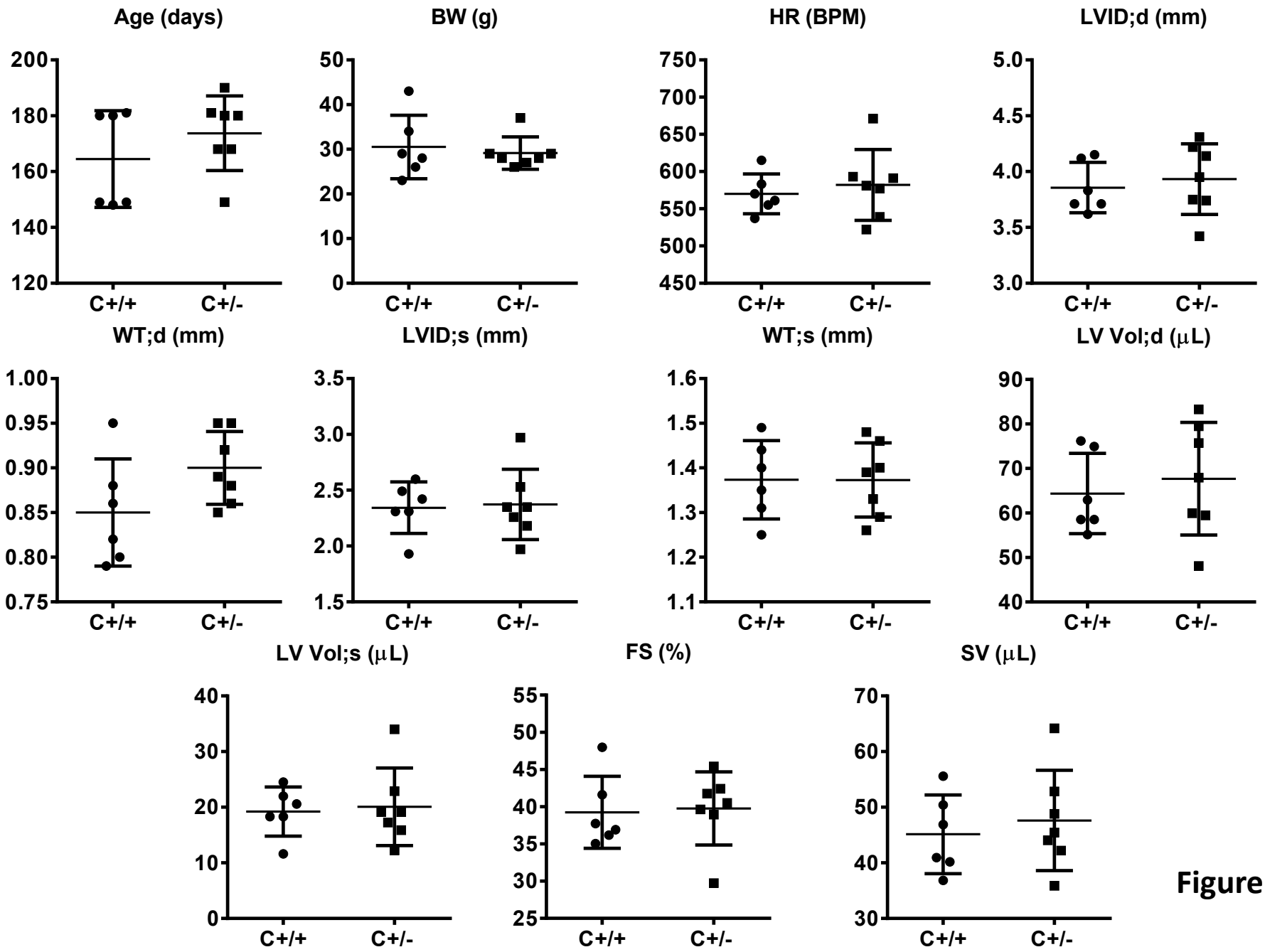

Figure S9

Tissue Morphometry of ~6mo old conscious male *α-MHC-Cre; cRbm20$^{\Delta RRM}$* mice (from Table S2c)

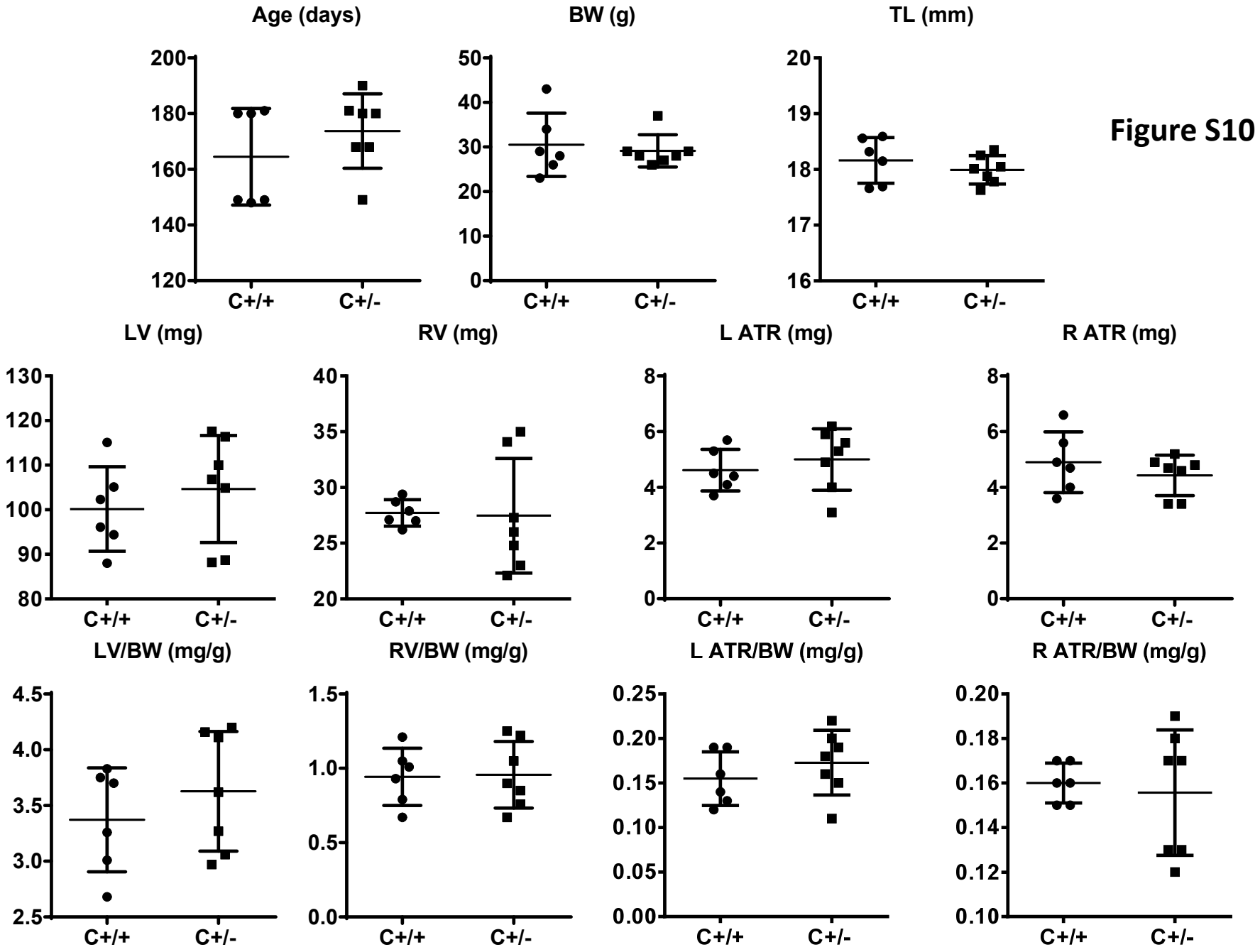

Figure S10

Cont. Tissue Morphometry of conscious male *α-MHC-Cre; cRbm20$^{\Delta RRM}$* mice (from Table S2c)

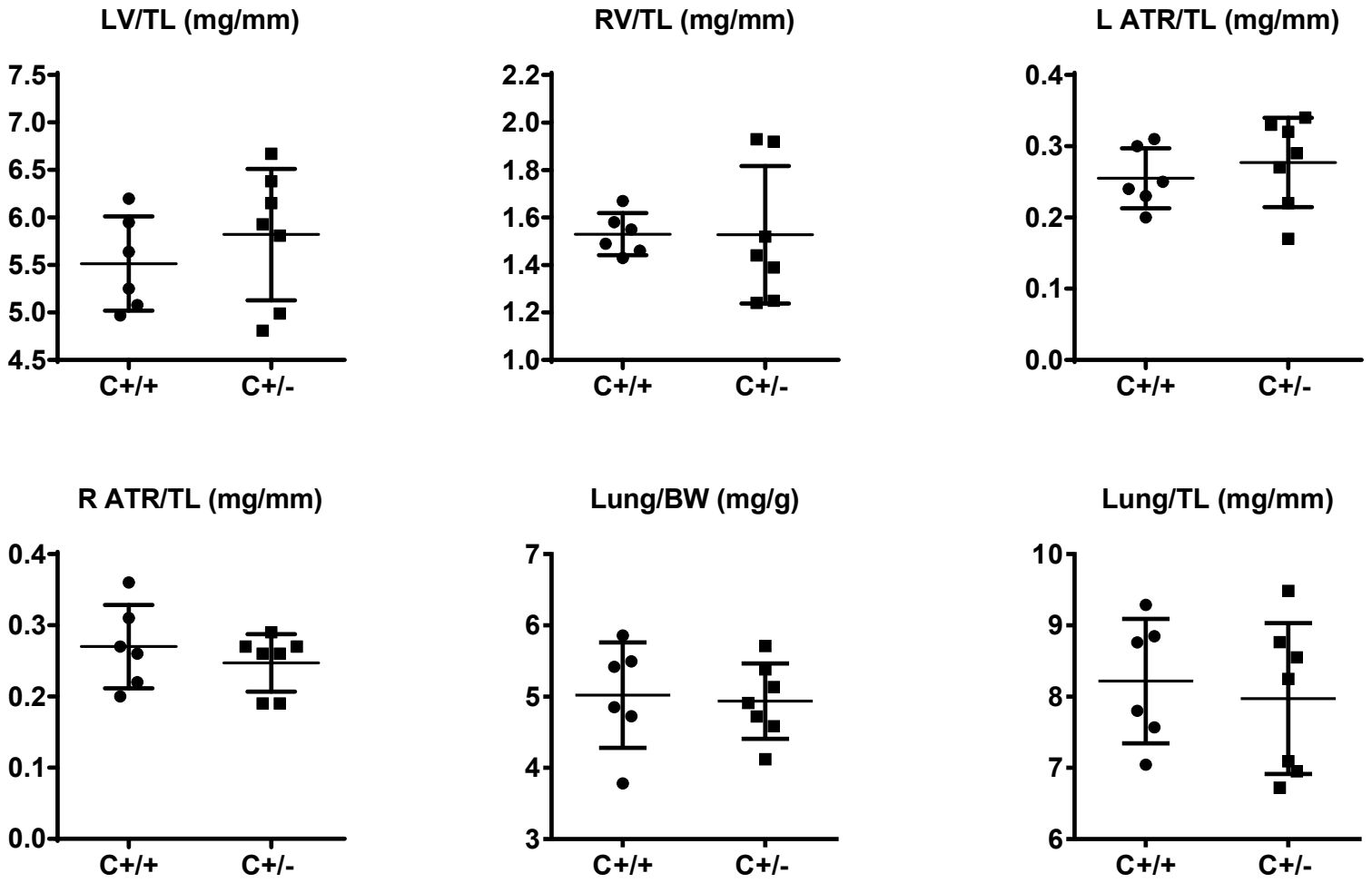

Figure S11

Legends to Supplemental Figures.

Figure S1. Generation of mice lacking RBM20's RNA Recognition Motif (RRM). A) Targeting vector design resulting in an in-frame deletion of the RRM encoded by exons 6 and 7. Details in Supplemental Methods. B) PCR analysis of expression of RBM20 exon 2 (not deleted) and RBM20 exon 6 (deleted). C) Western blot analysis with an antibody against RBM20's conserved N-terminus (outside the deleted region) shows expected expression patterns of wild-type RBM20 protein and higher mobility mutant RBM20 protein. D) Titin exon microarray analysis in *Rbm20*$^{\Delta RRM}$ LV. Many exons encoding Ig domains are upregulated in both +/- and -/- LV while many more PEVK domains are incorporated in the -/- compared to +/- LV. E-G) Western blots probing titin expression in *Rbm20*$^{\Delta RRM}$ LV. Experiments with the 9D10 antibody that recognizes repeating sequences within the PEVK element confirm upregulation of PEVK exons(E). Antibodies against cardiac titin's N2B spring element (exon 49) and cardiac titin's N2A element (exons 102-19) showed that the large titins expressed in *Rbm20*$^{\Delta RRM}$ mice are of the N2BA type (F). We also studied the Novex-III exon (exon 48) and found that it is not incorporated in the giant titins of the *Rbm20*$^{\Delta RRM}$ mouse (G). Instead the antibody detects the ~700 kDa novex-3 titin (a small titin isoform expressed at low levels[2]) with no differences amongst genotypes, indicating that RBM20 does not control splicing of novex-3 titin. *1D: 4 +/+ mice, 4 +/- mice and 4 -/- mice; 1E: 7 +/+ mice, 7 +/- mice and 9 -/- mice; 1F-G: 1 +/+ mouse, 1 +/- mouse and 1 -/- mouse.*

Figure S2a. Exon GeneChip microarray results identify titin gene (*Ttn*) as the predominant splicing target affected in left ventricular tissue. Pie charts at top show the distribution of exons affected in +/- (left) or -/- (right) for the *Rbm20*$^{\Delta RRM}$ mutation at the p<0.001 level. This platform confirms the observation with our custom array that exons encoding the Ig domains of titin are more sensitive to RBM20 dose than the PEVK exons; Ig domains 28-67 are incorporated in both +/- and -/- hearts while many more PEVK domains are incorporated in the -/- than+/- hearts. Supplemental Excel spreadsheets provide more details in exon level and gene level changes. There were no changes in gene expression level at p≤0.01. *2a: 3 +/+ mice, 3 +/- mice and 3 -/- mice.*

Figure S2b. **Multiple genes that are alternatively spliced in the mutant rat are unaltered in the *Rbm20*$^{\Delta RRM}$ mouse.** Endpoint RT-PCR analysis confirms that the spontaneous rat mutation in *Rbm20* resulted in deletion of all but the first exon removing all *Rbm20* function and that the targeted mouse *Rbm20*$^{\Delta RRM}$ deletion only removes exons 6-7. RT-PCR comfirms changes in splicing in *Rbm20mut* rats for *Cypher/Ldb3*, *CaMKIId* , *CaMKIIg*, *Sh3kbp*, *Sorbs1* and *Trdn*. In the *Rbm20*$^{\Delta RRM}$ -/- mice a similar change in *CaMKIId* splicing occurs as seen in *Rbm20mut* rats. Mouse *Cypher/Ldb3* shows a change in isoform ratio in *Rbm20*$^{\Delta RRM}$ -/- to make it more similar to what is seen in wild-type rats. The rat RBM20-targets: *CaMKIIg*, *Sh3kbp*, *Sorbs1* and *Trdn* show no change in splicing in the *Rbm20*$^{\Delta RRM}$ mouse model. *2b: 3+/+ rats, 3-/- rats, 3 +/+ mice, 3 +/- mice and 3 -/- mice.*

Figure S2c. **CaMKIIδ protein levels (A) and analysis of CaMKIIδ downstream targets (B-D) in *Rbm20*$^{\Delta RRM}$ mouse model.** No changes are found in the protein levels of total CaMKIIδ (A) and its downstream target p53 (D). No changes are found in the phosphorylation levels of the downstream targets T17 of PLB(B) and S282 of cMyBP-C (C). *S2c A: 7 +/+ mice, 7 +/- mice and 7 -/- mice; S2c B: 4 +/+ mice, 4+/- mice and 4 -/- mice; S2c C: 6+/+ mice, 7+/- mice and 10 -/- mice; S2c D: 8+/+ mice, 8+/- mice and 8 -/- mice.*

Figure S3. *Cypher* is alternatively spliced in *Rbm20*$^{\Delta RRM}$ mice. Western blot analysis of long and short cardiac Cypher isoforms reveals a decreased expression of the cardiac short isoform in the hearts of +/- and -/- mice. *S3A and B: 7 +/+ mice, 7 +/- mice and 7 -/- mice.*

Figure S4a. Ca^{2+} handling of *Rbm20*$^{\Delta RRM}$ cardiocytes. A and B) Fura-2 340/380 ratio of isolated intact cardiomyocytes stimulated at 2 Hz. Twitch amplitude and baseline signal (A) as well as maximal velocities of rising and decaying signal (B) are not different. C) Representative western blots of NCX-1, SERCA2a, and PLB (monomeric form) normalized by SERCA2a expression. There are no significant changes. *S4a A and B: 6 +/+ mice, 5 +/- mice and 5 -/- mice; S4a C: 5 +/+ mice, 5 +/- mice and 5 -/- mice.*

Figure S4a. Ca^{2+} handling of *Rbm20*$^{\Delta RRM}$ cardiocytes. A and B) Fura-2 340/380 ratio of isolated intact cardiomyocytes stimulated at 2 Hz. Twitch amplitude and baseline signal (A) as well as maximal velocities of rising and decaying signal (B) are not different. C) Representative western blots of NCX-1, SERCA2a, and PLB (monomeric form) normalized by SERCA2a expression. There are no significant changes. *S4a A and B: 6 +/+ mice, 5 +/- mice and 5 -/- mice; S4a C: 5 +/+ mice, 5 +/- mice and 5 -/- mice.*

Figure S4c. Shortening of unloaded intact cells beating at 2 Hz. A) End-Diastolic SL (SLd) and End-Systolic SL (SLs) of +/+, +/- and -/- *Rbm20*$^{\Delta RRM}$ cells. B) Shortening amplitude of +/- and -/- cells is larger than of +/+ cells, which is mostly due to their larger SLd. C) and D) Maximal departure and maximal return velocity are higher in -/- mice. *S4c: 7 +/+ mice, 6 +/- mice and 8 -/- mice.*

An explanation for the larger shortening amplitude of +/- and -/- *Rbm20*$^{\Delta RRM}$ cells is the titin-based *restoring* force against which unloaded cells have to shorten (this is a negative force that is present below the slack length of cells and that pushes out on the Z-disks). Restoring force scales with the fractional extension of titin's extensible region and for a given sarcomere length below the slack length the restoring force will be less in +/- and -/- cells than in wt cells. Consistent with this is the higher maximal departure velocity of unloaded beating +/- myocytes (Panel C). (The increased maximum return velocity of -/- cells in panel D can not be explained by restoring force differences. Considering that the maximum return velocity is reached while the calcium transient has decayed to only ~ 50% of

its peak (results not shown) the increased max return velocity of -/- cells might be due to their lower calcium sensitivity).

Figure S4d. Cell dimensions of skinned cardiocytes. Cell were imaged perpendicular to their long axis. Thickness /width ratio is significantly increased in -/- cells. Cross-sectional area is unaltered. *S4d: 10 +/+ mice, 10 +/- mice and 9 -/- mice.*

Figure S5. Ca^{2+} transient before and after 10% length change. A) Simultaneous recording of SL and Fura-2 (340/380 ratio) in intact cardiomyocytes. B) Transient amplitudes of the last twitch at baseline (pre-stretch twitch) versus the immediate twitch after 10% stretch (post-stretch twitch) were not different. *7 cells +/+, 14 cells +/- and 19 cells -/-.*

Figure S6. Myofilament protein analysis in LV. A and B) Representative Coommassie blue and Pro-Q Diamond stained gel. There are no noticeable differences in the phosphorylation level of the myofilament proteins amongst the three groups. C) Myosin heavy chain (MHC) expression. A 1-day old neonatal sample (ctrl) is shown for reference as it expresses both □-MHC and □-MHC. There is no detectable change in MHC isoform expression in the three groups. D) Regulatory proteins expression and specific phosphorylation sites. pS282 cMyBP-C was normalized by total cMyBP-C, cTnT, and TM with actin as a loading control; pS23/24 cTnI was normalized by total cTnI and MLC2v with GAPDH as a loading control. There are no significant differences amongst the three groups. *S6C: 3 +/+ mice, 3 +/- mice and 3 -/- mice; S6D: 4 +/+ mice, 4 +/- mice and 4 -/- mice.*

Supplemental Table Captions

Table S1a. Echocardiography of LV systolic function of ~20 months old anesthetized female *Rbm20*$^{\Delta RRM}$ mice. Abbreviations: BW: body weight; HR: heart rate; BPM: beats per minute; LV: left ventricle; LVIDd: left ventricular internal diastolic diameter; WTd: diastolic wall thickness; LVIDs; left ventricular internal systolic diameter; WTs: systolic wall thickness; Eccentricity: LVIDd/WTd; LA: left atrium; LV Vold: left ventricular diastolic volume; LV Vols: left ventricular systolic volume; EF: ejection fraction; FS: fractional shortening.

Table S1b. Tail cuff blood pressure measurement in conscious male *Rbm20*$^{\Delta RRM}$ mice. None of the measured parameters are significantly different.

Table S1c. Conscious mouse echocardiography of ~ 4 months old male *Rbm20*$^{\Delta RRM}$ mice. Conscious M-mode echos were obtained in restrained mice using a parasternal short-axis view at the level of the papillary muscles. Abbreviations: BW: body weight; HR: heart rate; BPM: beats per minute; LV: left ventricle; LVIDd: left ventricular internal diastolic diameter; WTd: diastolic wall thickness; LVIDs; left ventricular internal systolic diameter; WTs: systolic wall thickness; Eccentricity: LVIDd/WTd; LV Vold: left ventricular diastolic volume; LV Vols: left ventricular systolic volume; FS: fractional shortening.; SV: stroke volume. **p<0.01 vs WT (+/+); # p<0.05 vs het (+/-).

Table S1d. Echocardiography of ~6 months old anesthetized male *α-MHC-Cre; cRbm20*$^{\Delta RRM\ flox/+}$ mice. Abbreviations: C+/+: WT; C+/-: one allele with floxed RRM and one allele WT; BW: body weight; LV: left ventricle; LVIDd: left ventricular internal diastolic diameter; WTd: diastolic wall thickness; LVIDs; left ventricular internal systolic diameter; WTs: systolic wall thickness; Eccentricity: LVIDd/WTd; LA: left atrium; LV Vold: left ventricular diastolic volume; LV Vols: left ventricular systolic volume; EF: ejection fraction; FS: fractional shortening.; SV: stroke volume. MV decal time: mitral valve E-wave deceleration time . * p<0.05 vs WT (+/+).

Table S1e. Conscious echocardiography of ~6 months old male *α-MHC-Cre; cRbm20*$^{\Delta RRMflox/+}$ mice. Conscious M-mode echos were obtained in restrained mice using a parasternal short-axis view at the level of the papillary muscles. Abbreviations: C+/+: WT; C+/-: one allele with floxed RRM and one allele WT; BW: body weight; HR: heart rate; BPM: beats per minute; LV: left ventricle; LVIDd: left ventricular internal diastolic diameter; WTd: diastolic wall thickness; LVIDs; left ventricular internal systolic diameter; WTs: systolic wall thickness; Eccentricity: LVIDd/WTd; LV Vold: left ventricular diastolic volume; LV Vols: left ventricular systolic volume; FS: fractional shortening.; SV: stroke volume.

Table S2a. Tissue morphometric study of male and female ~4 months old *Rbm20*$^{\Delta RRM}$ mice. BW: body weight; HW: whole heart weight; LV: left ventricle; RV: right ventricle; ATR: left and right atria; TL: tibial length.

Table S2b. Tissue morphometric study of ~20 months old female *Rbm20*$^{\Delta RRM}$ mice. Abbreviations: see caption for Table S2a. ATR: atria.

Table S2c. Tissue morphometric study of ~6 months old male *α-MHC-Cre; cRbm20*$^{\Delta RRMflox/+}$ mice. Abbreviations: see caption for Table S2a. ATR: atria. No significant changes were found in C+/- mice.

Table S3. Pressure (P)-volume (V) analysis. PV analysis was performed on lightly anesthetized and ventilated 4 months old male mice using 1.5% isoflurane. Body temperature was maintained at 37 °C and a 1.2F PV catheter was introduced retrograde into the LV through the left carotid artery. All measurements were obtained during a pause in ventilation. Inferior venal caval occlusions were performed to assess load-independent parameters. Abbreviations: see caption for Tables S1-S3; Additionally, ESP: end-systolic pressure; EDP: end-diastolic pressure; ESV: end-systolic volume; EDV: end-diastolic volume; EF: ejection fraction; Ea: effective arterial elastance; Ees: end-systolic elastance; V0: volume at which there is 0 mmHg pressure in the left ventricle. This is the x-axis intercept of the linear fit of the end-systolic elastance (Ees). EDPVR: end-diastolic PV relationship.

Table S4. Systolic function of intact cardiomyocytes. FSM of intact cells was calculated from the slope of the systolic stress-systolic SL relation and systolic stress-diastolic SL relation. Bottom of table shows that maximal active stress of skinned cardiac myocytes was reduced in -/- cells (relative to +/+ cells) by 27%. FSM of -/- was corrected for this percent reduction.

Table S5. Contractility measurements in LV papillary muscle of *Rbm20*$^{\Delta RRM}$ mice. * significance vs. -/- at same SL (ANOVA); # significance vs. +/- at same SL (ANOVA). SL: sarcomere length (mm); BL= sarcomere length of slack preparation. LDA: length dependent activation obtained from fitting the pCa50-SL relation of each muscle strip (units pCa/μm sarcomere). F_{max}; tension at pCa 4.5 (in mN/mm2). Tension cost: ATPase rate/tension (in pmol/(mm mN s). ND: not determined. K_{tr}: rate constant of tension redevelopment following rapid release-restretch (in s-1).

REFERENCES

1. Gyurko R, Kuhlencordt P, Fishman MC, Huang PL. Modulation of mouse cardiac function in vivo by enos and anp. *American journal of physiology. Heart and circulatory physiology*. 2000;278:H971-981
2. Lahmers S, Wu Y, Call DR, Labeit S, Granzier H. Developmental control of titin isoform expression and passive stiffness in fetal and neonatal myocardium. *Circulation research*. 2004;94:505-513
3. Hidalgo C, Hudson B, Bogomolovas J, Zhu Y, Anderson B, Greaser M, Labeit S, Granzier H. Pkc phosphorylation of titin's pevk element: A novel and conserved pathway for modulating myocardial stiffness. *Circulation research*. 2009;105:631-638, 617 p following 638
4. Warren CM, Jordan MC, Roos KP, Krzesinski PR, Greaser ML. Titin isoform expression in normal and hypertensive myocardium. *Cardiovascular research*. 2003;59:86-94
5. Hudson BD, Hidalgo CG, Gotthardt M, Granzier HL. Excision of titin's cardiac pevk spring element abolishes pkcalpha-induced increases in myocardial stiffness. *Journal of molecular and cellular cardiology*. 2010;48:972-978
6. Guo W, Schafer S, Greaser ML, Radke MH, Liss M, Govindarajan T, Maatz H, Schulz H, Li S, Parrish AM, Dauksaite V, Vakeel P, Klaassen S, Gerull B, Thierfelder L, Regitz-Zagrosek V, Hacker TA, Saupe KW, Dec GW, Ellinor PT, MacRae CA, Spallek B, Fischer R, Perrot A, Ozcelik C, Saar K, Hubner N, Gotthardt M. Rbm20, a gene for hereditary cardiomyopathy, regulates titin splicing. *Nature medicine*. 2012;18:766-773
7. Freiburg A, Trombitas K, Hell W, Cazorla O, Fougerousse F, Centner T, Kolmerer B, Witt C, Beckmann JS, Gregorio CC, Granzier H, Labeit S. Series of exon-skipping events in the elastic spring region of titin as the structural basis for myofibrillar elastic diversity. *Circulation research*. 2000;86:1114-1121
8. Wang SM, Greaser ML. Immunocytochemical studies using a monoclonal antibody to bovine cardiac titin on intact and extracted myofibrils. *Journal of muscle research and cell motility*. 1985;6:293-312
9. Bang ML, Centner T, Fornoff F, Geach AJ, Gotthardt M, McNabb M, Witt CC, Labeit D, Gregorio CC, Granzier H, Labeit S. The complete gene sequence of titin, expression of an unusual approximately 700-kda titin isoform, and its interaction with obscurin identify a novel z-line to i-band linking system. *Circulation research*. 2001;89:1065-1072
10. Reiser PJ, Kline WO. Electrophoretic separation and quantitation of cardiac myosin heavy chain isoforms in eight mammalian species. *The American journal of physiology*. 1998;274:H1048-1053
11. Chung C, Granzier H. Dissection of determinants of passive pressure and measurement of sarcomere length in the mouse left ventricle. *Journal of Molecular and Cellular Cardiology*. 2011;50:731-739
12. Granzier HL, Radke MH, Peng J, Westermann D, Nelson OL, Rost K, King NM, Yu Q, Tschope C, McNabb M, Larson DF, Labeit S, Gotthardt M. Truncation of titin's elastic pevk region leads to cardiomyopathy with diastolic dysfunction. *Circulation research*. 2009;105:557-564
13. Radke MH, Peng J, Wu Y, McNabb M, Nelson OL, Granzier H, Gotthardt M. Targeted deletion of titin n2b region leads to diastolic dysfunction and cardiac atrophy. *Proceedings of the National Academy of Sciences of the United States of America*. 2007;104:3444-3449
14. Granzier H, Labeit S. Structure-function relations of the giant elastic protein titin in striated and smooth muscle cells. *Muscle & nerve*. 2007;36:740-755
15. Labeit S, Lahmers S, Burkart C, Fong C, McNabb M, Witt S, Witt C, Labeit D, Granzier H. Expression of distinct classes of titin isoforms in striated and smooth muscles by alternative splicing, and their conserved interaction with filamins. *Journal of molecular biology*. 2006;362:664-681

16. Chung CS, Hutchinson KR, Methawasin M, Saripalli C, Smith JE, 3rd, Hidalgo CG, Luo X, Labeit S, Guo C, Granzier HL. Shortening of the elastic tandem immunoglobulin segment of titin leads to diastolic dysfunction. *Circulation*. 2013;128:19-28
17. Greer KA, McReynolds MR, Brooks HL, Hoying JB. Carma: A platform for analyzing microarray datasets that incorporate replicate measures. *BMC Bioinformatics*. 2006;7:149
18. Gellert P, Uchida S, Braun T. Exon array analyzer: A web interface for affymetrix exon array analysis. *Bioinformatics*. 2009;25:3323-3324
19. Clark TA, Schweitzer AC, Chen TX, Staples MK, Lu G, Wang H, Williams A, Blume JE. Discovery of tissue-specific exons using comprehensive human exon microarrays. *Genome biology*. 2007;8:R64
20. Zhang B, Kirov S, Snoddy J. Webgestalt: An integrated system for exploring gene sets in various biological contexts. *Nucleic acids research*. 2005;33:W741-748
21. Wang J, Duncan D, Shi Z, Zhang B. Web-based gene set analysis toolkit (webgestalt): Update 2013. *Nucleic acids research*. 2013;41:W77-83
22. O'Connell TD, Rodrigo MC, Simpson PC. Isolation and culture of adult mouse cardiac myocytes. *Methods in molecular biology*. 2007;357:271-296
23. Irving TC, Konhilas J, Perry D, Fischetti R, de Tombe PP. Myofilament lattice spacing as a function of sarcomere length in isolated rat myocardium. *American journal of physiology. Heart and circulatory physiology*. 2000;279:H2568-2573
24. Yasuda SI, Sugiura S, Kobayakawa N, Fujita H, Yamashita H, Katoh K, Saeki Y, Kaneko H, Suda Y, Nagai R, Sugi H. A novel method to study contraction characteristics of a single cardiac myocyte using carbon fibers. *American journal of physiology. Heart and circulatory physiology*. 2001;281:H1442-1446
25. Iribe G, Helmes M, Kohl P. Force-length relations in isolated intact cardiomyocytes subjected to dynamic changes in mechanical load. *American journal of physiology. Heart and circulatory physiology*. 2007;292:H1487-1497
26. Granzier HL, Irving TC. Passive tension in cardiac muscle: Contribution of collagen, titin, microtubules, and intermediate filaments. *Biophysical journal*. 1995;68:1027-1044
27. Farman GP, Tachampa K, Mateja R, Cazorla O, Lacampagne A, de Tombe PP. Blebbistatin: Use as inhibitor of muscle contraction. *Pflugers Archiv : European journal of physiology*. 2008;455:995-1005
28. Helmes M, Trombitas K, Granzier H. Titin develops restoring force in rat cardiac myocytes. *Circulation research*. 1996;79:619-626
29. Burkhoff D, Mirsky I, Suga H. Assessment of systolic and diastolic ventricular properties via pressure-volume analysis: A guide for clinical, translational, and basic researchers. *American journal of physiology. Heart and circulatory physiology*. 2005;289:H501-512
30. Stewart JA, Jr., Wei CC, Brower GL, Rynders PE, Hankes GH, Dillon AR, Lucchesi PA, Janicki JS, Dell'Italia LJ. Cardiac mast cell- and chymase-mediated matrix metalloproteinase activity and left ventricular remodeling in mitral regurgitation in the dog. *Journal of molecular and cellular cardiology*. 2003;35:311-319
31. Magid A, Law DJ. Myofibrils bear most of the resting tension in frog skeletal muscle. *Science*. 1985;230:1280-1282
32. Granzier HL, Burns DH, Pollack GH. Sarcomere length dependence of the force-velocity relation in single frog muscle fibers. *Biophysical journal*. 1989;55:499-507
33. Fabiato A, Fabiato F. Calculator programs for computing the composition of the solutions containing multiple metals and ligands used for experiments in skinned muscle cells. *Journal de physiologie*. 1979;75:463-505

34. Konhilas JP, Maass AH, Luckey SW, Stauffer BL, Olson EN, Leinwand LA. Sex modifies exercise and cardiac adaptation in mice. *American journal of physiology. Heart and circulatory physiology*. 2004;287:H2768-2776